LANL Ref

JOURNAL OF GEOPHYSICAL RESEARCH, VOL. 105, NO. D17, PAGES 22,147–22,166, SEPTEMBER 16, 2000

Measurements of excess O_3, CO_2, CO, CH_4, C_2H_4, C_2H_2, HCN, NO, NH_3, HCOOH, CH_3COOH, HCHO, and CH_3OH in 1997 Alaskan biomass burning plumes by airborne Fourier transform infrared spectroscopy (AFTIR)

Jon G. Goode[1] and Robert J. Yokelson

Department of Chemistry, University of Montana, Missoula

Darold E. Ward, Ronald A. Susott, Ronald E. Babbitt, Mary Ann Davies, and Wei Min Hao

Rocky Mountain Research Station, U. S. Department of Agriculture Forest Service, Missoula, Montana

Abstract. We used an airborne Fourier transform infrared spectrometer (AFTIR), coupled to a flow-through, air-sampling cell, on a King Air B-90 to make in situ trace gas measurements in isolated smoke plumes from four, large, boreal zone wildfires in interior Alaska during June 1997. AFTIR spectra acquired near the source of the smoke plumes yielded excess mixing ratios for 13 of the most common trace gases: water, carbon dioxide, carbon monoxide, methane, nitric oxide, formaldehyde, acetic acid, formic acid, methanol, ethylene, acetylene, ammonia and hydrogen cyanide. Emission ratios to carbon monoxide for formaldehyde, acetic acid, and methanol were 2.2 ± 0.4%, 1.3 ± 0.4%, and 1.4 ± 0.1%, respectively. For each oxygenated organic compound, a single linear equation fits our emission factors from Alaska, North Carolina, and laboratory fires as a function of modified combustion efficiency (MCE). A linear equation for predicting the NH_3/NO_x emission ratio as a function of MCE fits our Alaskan AFTIR results and those from many other studies. AFTIR spectra collected in downwind smoke that had aged 2.2 ± 1 hours in the upper, early plume yielded $\Delta O_3/\Delta CO$ ratios of 7.9 ± 2.4% resulting from O_3 production rates of ~50 ppbv h^{-1}. The $\Delta NH_3/\Delta CO$ ratio in another plume decreased to $1/e$ of its initial value in ~2.5 hours. A set of average emission ratios and emission factors for fires in Alaskan boreal forests is derived. We estimate that the 1997 Alaskan fires emitted 46 ± 11 Tg of CO_2.

1. Introduction

Biomass burning is a major source of trace gases for the global atmosphere [*Crutzen and Andreae*, 1990]. About 80% of biomass burning is thought to occur in the tropics [*Hao and Liu*, 1994]. Fires are also common in the boreal zone, but less is known about their atmospheric impacts. The boreal zone lies between 45° and 70°N latitude and includes an estimated 1.2 billion ha of mostly coniferous forest. This represents about 30% of the global forested area [*FIRESCAN Science Team*, 1996]. The low average temperatures in the boreal region slow both growth and decomposition. Estimates compiled by *Smith et al.* [1993] and *Apps et al.* [1993] suggested that ~40% of the global, terrestrial, plant-derived carbon is contained in the boreal zone as follows: 3% (64 Pg) in live plant biomass, 12% (231 Pg) in detritus and forest soils, and 22% (419 Pg) in colocated peat deposits.

Fire is the major, natural disturbance in boreal ecosystems [*FIRESCAN Science Team*, 1996]. *Kasischke et al.* [1999] recently estimated that ~8.8 million ha of the global boreal forest burn annually with considerable interannual variation. Severe drought can be associated with a large increase in burned area for extensive regions within the boreal zone. For instance, *Cahoon et al.* [1994, 1996] estimated the burned area for the East Asian boreal forest to be 1.5 million ha in 1992 and 14.5 million ha in 1987. Thus the total, boreal forest burned area, in episodic years, may be 15-20 million ha [*Kasischke et al.*, 1999]. In addition, average fuel consumption can increase in drought-affected regions as conditions that allow crown fires to develop can prevail for longer periods and organic soils (peat, duff, etc.) can ignite and burn to considerable depth. Because of this sensitivity, it is significant that fire may already be increasing in boreal forests in response to global warming. According to *Kasischke et al.* [1999], the average, annual area burned in the North American boreal forest rose from 1.5 million ha in the 1970s to 3.2 million ha in the 1990s coincident with a 1°-1.6°C rise in average annual temperature in the region. Under a doubled CO_2 scenario, global circulation models projected (on average) a 4°-6°C rise in summer temperatures and a simultaneous decrease in soil moisture for much of Canada and Russia [*Stocks et al.*, 1998]. Studies by *Flannigan and Van Wagner* [1991] and *Wotton and Flannigan* [1993] predicted that, across Canada, a 2 × CO_2 scenario would increase fire danger by 50% and the length of the fire season by 30 days.

[1]Now at Bruker Optics, Inc., Billerica, Massachusetts.

This paper is not subject to U. S. copyright. Published in 2000 by the American Geophysical Union.

Paper number 2000JD900287.

9813

Only a few studies have characterized the emissions from boreal fires. *Nance et al.* [1993] reported airborne measurements of the emission factors for CO_2, CO, CH_4, C_2H_6, C_2H_2, C_3H_8, C_3H_6, nonmethane hydrocarbons (C_2-C_{10}, excluding ethene), N_2O, NH_3, NO_x, and particulate matter for a single fire burning in an Alaskan black spruce forest. *Hegg et al.* [1990] and *Radke et al.* [1991] reported a similar suite of measurements for three boreal forest fires in Ontario, Canada. On one of these fires, *Susott et al.* [1991] also measured the fire-integrated CO_2 and CO emission factors using tower-based instruments. *Cofer et al.* [1998] compared spot measurements of CO_2, CO, CH_4, H_2, and total nonmethane hydrocarbons obtained during several Canadian slash fires with similar measurements obtained during prescribed crown fires in Canada and Russia [*Cofer et al.*, 1989, 1996]. *Yokelson et al.* [1997] measured the emission factors for CO_2, CO, CH_4, C_2H_4, C_2H_2, C_3H_6, HCHO, $CHOCH_2OH$, CH_3OH, C_6H_5OH, CH_3COOH, HCOOH, NH_3, HCN, and carbonyl sulfide (OCS) from smoldering combustion of organic soils obtained in central Alaska. We now report airborne measurements carried out in June 1997 of the emission factors for 12 trace gases from four Alaskan fires. These fires (taken together) eventually contributed almost 40% to the total area burned in Alaska that year.

We obtained the results in this paper using our airborne Fourier transform infrared (AFTIR) trace gas measurement system. We had earlier developed the use of ground-based, open-path FTIR to characterize fire emissions, because it provided an overview of the reactive and stable gases present above several ppbv in smoke [*Griffith et al.*, 1991; *Yokelson et al.*, 1996a, 1996b, 1997, 1998; *Goode et al.*, 1999]. Our ground-based studies were mainly of biomass fires in the U. S. Department of Agriculture Forest Service, Fire Sciences Laboratory combustion facility where we could ensure representative, fire-integrated sampling. We developed a set of linear equations based on our laboratory results to predict the emissions of individual oxygenated organic compounds (HCHO, CH_3OH, CH_3COOH, etc.) as a function of the modified combustion efficiency (MCE) of a fire. We found that fires are a major source of many oxygenated compounds, which are important in the atmosphere as secondary HO_x sources [*Yokelson et al.*, 1996b, 1997, 1999]. We also showed that a simple linear equation fit the NH_3/NO_x emission ratio as a function of MCE [*Yokelson et al.*, 1996b; *Goode et al.*, 1999]. (NH_3 and NO_x are the major, reactive, nitrogen-containing emissions from fires.) We developed AFTIR (an airborne FTIR coupled to a flow-through multipass cell) because of the importance of sampling real fires, the need to confirm the relevance of our laboratory studies, and our interest in downwind plume chemistry.

Our first deployment of AFTIR was on fires in North Carolina during April 1997. We measured emissions on three field fires that were very similar to the emissions we had measured previously in laboratory studies [*Yokelson et al.*, 1999]. This confirmed that the convection column above a fire could draw in the products of flaming and smoldering combustion and confirmed the relevance of our extensive laboratory emission factor measurements. During the North Carolina study we measured emission factors for prescribed fires in the southeastern United States, which is an important type of biomass burning on the national scale. However, we were unable to sample downwind of those fires due to airspace restrictions.

The primary goals of the study reported here were to (1) obtain an expanded range of field results to further challenge and develop the emission-prediction equations (described above) that were based mostly on our laboratory data, (2) probe downwind plume chemistry, and (3) extensively characterize the emissions from fires in interior Alaska, which contains 52 million ha of the globally important boreal ecosystems [*Birdsey*, 1992]. In this paper we describe the fires we sampled and our measurement methodology. We present field results that support our simple models for production of oxygenated organic compounds and nitrogen-containing compounds. We present our first spot measurements of the rate of downwind O_3 production and ammonia loss. Finally, we derive a set of average emission factors for Alaskan, boreal forest fires and estimate the total trace gas emissions at various scales within the boreal zone.

2. Experimental Methods

2.1. Fire Descriptions

The Alaskan fire season usually starts in May and can last until October. Due to large interannual variation in weather, the annual area burned has ranged from ~16,000 to ~1,260,000 ha over the last 10 years. The 1997 Alaska fire season was typical in that several very large wildfires, ignited by lightning, accounted for most of the area burned [*Office of Fire and Aviation Management*, 1998]. Figure 1 shows a map of Alaska with the location and extent of the 1997 fires > 40 ha, which accounted for nearly all the ~754,000 ha burned [*Alaska Fire Service*, 1997]. We sampled fires in Alaska during the second half of June, which included the warmest 7-day period of 1997 (in Fairbanks) and came toward the end of ~3 months of above normal temperatures without significant precipitation. Thus we probably sampled the type of fires that produce much of the total emissions. We sampled four wildfires, designated B320, B280, B349, and B309 by the Alaska Fire Service (see Figure 1) during six flight missions. More details about these fires are given below. Throughout this paper we refer to the individual wildfires by their Alaska Fire Service (AFS) designated fire number and all altitudes are referenced to ground level.

2.1.1. Wildfire B320. Wildfire B320 burned in a mixture of grasses and low shrubs and was probably started by lightning during the evening of June 12. The fire was located at 64° 02' N, 146° 20' W longitude, ~115 km southeast of Fairbanks (Figure 1), in the Fort Greely Military Firing Range. B320 was a slow-moving surface fire that had burned ~61 ha when we began sampling on June 13 at ~1400 local time (LT). A 4 ± 1 m s^{-1} southwesterly wind had established a weak, wind-driven smoke plume with a maximum altitude of ~600 m. The surface temperature was 20°C and the relative humidity (RH) ~30%. Cloud cover was broken at 6100 m and the temperature lapse rate (at Fairbanks) was -7.3°C km^{-1} up to ~10 km. Four smoke samples were collected directly above the source of the smoke. The fire was declared out on June 26 having burned ~1010 ha. AFS fire history data showed that the southern half of this fire also burned during 1996 and 1956 and that the whole area burned in 1990. The frequent fires and bombing range activity probably promoted the dominance of the site by grasses and low shrubs.

2.1.2. Wildfire B280. Wildfire B280 was started by lightning on June 7 in the Innoko Wildlife Refuge ~ 130 km south of Galena (Figure 1). Our first flight to this fire was

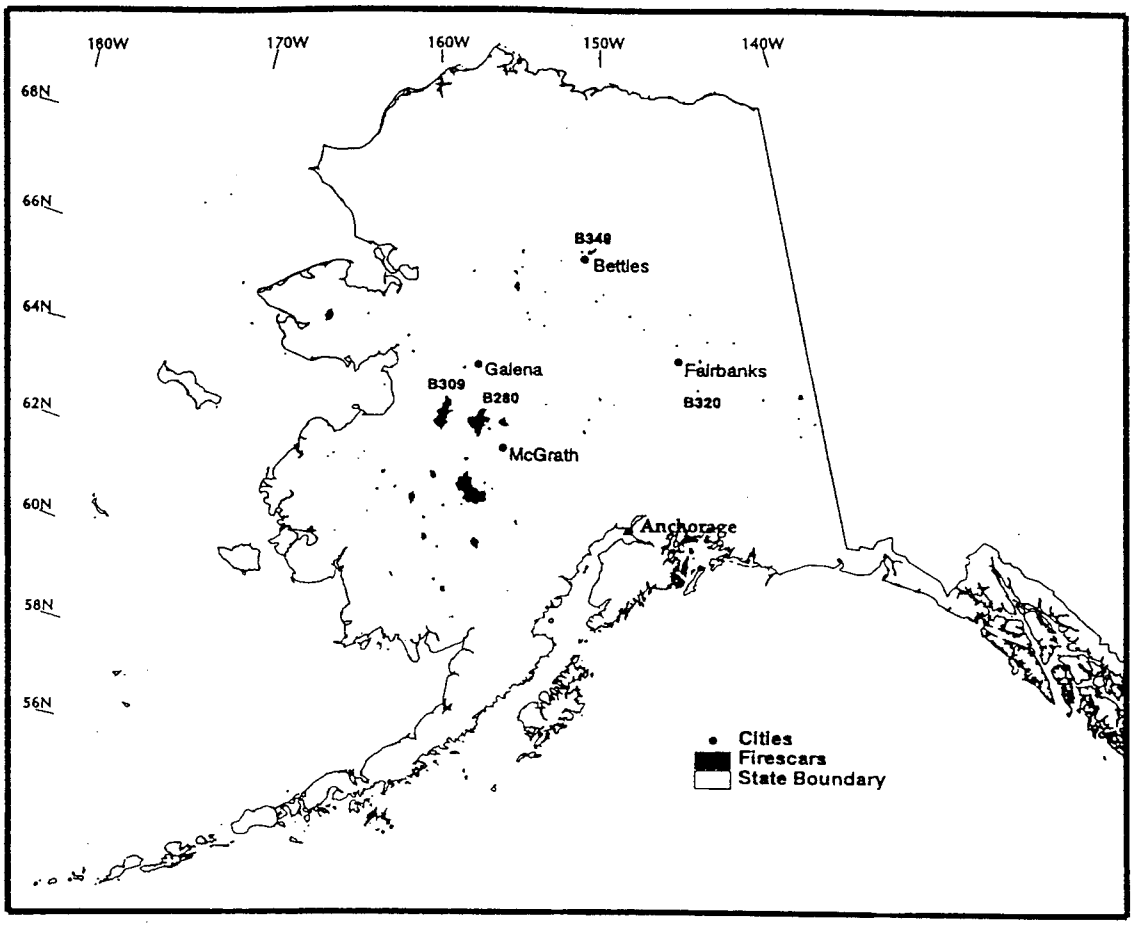

Figure 1. A map of Alaska showing the 1997 fires larger than 40 ha. The location of the four fires sampled in this work and the towns mentioned in the text are also indicated.

during the evening of June 21 when the fire had grown to ~1500 ha and was actively burning in an area centered on 63° 34' N, 157° 04' W. The fire front consisted of multiple fingers burning in a mosaic of black spruce, shrub, and bog. A 6 ± 1 m s^{-1} northwesterly wind had shaped a smoke plume that was ~6 km wide (at a point 11 km downwind and an altitude of ~600 m) and that ultimately reached a maximum altitude of ~1500 m. At ~1900 LT the surface temperature was ~16°C and the RH was ~56%. By ~2100 LT these had changed to ~14°C and ~63%. During this period the sky was overcast and the cloud level was ~2000 m. Four smoke samples were collected directly above the leading edge of the fire while five others were collected within ~13 km of the source at various altitudes.

We returned to this fire on June 23, in the late afternoon, when the fire had almost tripled in size to ~4340 ha and was rapidly spreading southward with 15 m flame lengths. The wind was from the north at 7.5 ± 1.5 m s^{-1} near the ground, but decreased to 5.5 ± 1.5 m s^{-1} at ~1600 m. Multiple, wind-driven smoke plumes converged downwind and leveled off at a maximum altitude of ~1700 m. Ten kilometers downwind from the fire front the combined smoke plume was ~15 km wide. The surface temperature was 25°C, RH ~28%, and the cloud cover was broken at ~7600 m. The lapse rate was -7.6°C km^{-1} up to ~11 km. Three smoke samples were collected directly above the fire front while six others were collected within ~12 km of the source at various altitudes. In addition, three downwind samples were collected as we flew ~50 km down the long axis of the plume (see section 3.4).

We last sampled this fire at ~1400 LT on June 24. The fire had continued to spread to the south and a northeasterly 3 ± 1 m s^{-1} wind had generated two active smoke plumes at either end of the main burning front. The surface temperature was 26°C, RH 35%, and cloud cover was broken at ~7600 m. The lapse rate was -7.4°C km^{-1} up to ~11 km. Two smoke samples were collected above the source before moving on to fire B309 (see section 2.1.4). Wildfire B280 was declared out on October 27 having burned a total of 148,062 ha.

2.1.3. Wildfire B349. Wildfire B349 was first reported on June 21 after a lightning storm. The fire was located at 67° 05' N, 151° 11' W, ~ 24 km northeast of Bettles (Figure 1). Our measurements began on the afternoon of June 22 when the fire had grown to ~250 ha and was aggressively spreading in black spruce on a ridge with torching of whole trees. The surface temperature was 23°C, RH 32%, and the wind was light and variable. Cloud cover was scattered at 2150 m. Seven smoke samples were collected within ~2 km of the head (leading edge) of the fire. The fire was declared out on July 23 having burned 9787 ha.

2.1.4. Wildfire B309. Wildfire B309 was first reported on June 10 burning in the Innoko Wildlife Refuge in an open black spruce forest/shrub/bog mosaic. The fire was located at 63° 38' N, 158° 25' W, ~64 km west of wildfire B280 (Figure 1). We began measurements on the afternoon of June 24 when

the fire had grown to ~2500 ha and was spreading fastest at both ends of the fire front. The smoke column rose to ~2300 m before leveling out under the influence of a 4 ± 1 m s^{-1} northeasterly wind. Five kilometers downwind the smoke column was ~10 km wide. The surface temperature was 27°C, RH 37%, and cloud cover was broken at 2750 m. The lapse rate was -7.4°C km^{-1} up to ~11 km. One smoke sample was collected directly above the head of the fire while three others were collected within ~4 km of the source at various altitudes.

We returned to the fire 3 days later (June 27) in the late afternoon when the fire had grown to ~8100 ha. The smoke plume rose to a maximum altitude of ~1850 m under the influence of a 7 ± 2 m s^{-1} northwesterly wind. The surface temperature was 24°C and RH ~42%. There were a few clouds at ~2000 m and the lapse rate was -7.5°C km^{-1} up to ~11 km. One smoke sample was collected directly above the head of the fire while two others were collected within ~17 km of the source. In addition, two smoke samples were collected as we flew ~60 km down the long axis of the smoke plume and one sample was collected while traversing the plume ~56 km downwind (see section 3.4). The fire was declared out on October 16 having burned 124,691 ha.

2.2. Measurement Strategy

Various configurations that can be used to perform airborne FTIR measurements were discussed by *Yokelson et al.* [1999]. In this work we acquired FTIR spectra of air samples in a cell inside the aircraft. Air samples flowed into the cell (driven by ram pressure) through an inlet (25 mm ID) mounted on the copilot's side window and approximately 1.5 m of Teflon tubing (17 mm ID). The cell's inlet and outlet lines were controlled by high-throughput, air/solenoid-actuated valves (Milwaukee Valve Co., Inc.) that allowed us to "grab" smoke or background air samples. In addition, simultaneously closing the inlet and outlet valves significantly reduced the noise in the important 900-1100 cm^{-1} region of the FTIR spectrum [*Yokelson et al.*, 1999]. The exhaust port was a Venturi design on the underside of the aircraft. The $1/e$ cell exchange time was 4-5 s. We reduced the small risk of sampling artifacts by coating all the sample intake surfaces and the metal surfaces in the cell with a nonreactive halocarbon wax [*Webster et al.*, 1994].

Infrared spectra of the cell contents were acquired continuously (every 1.7 s) throughout each flight and the flow control valves were normally open, which usually flushed the cell with background air. To collect smoke samples, we flew into the smoke plume and then closed the valves when the cell was well flushed with smoke. The valves remained closed for up to 10 min while spectra of the smoke sample were acquired. Next both valves were opened and the cell was flushed with background air for at least 30 s before the valves were closed again and spectra of the background air sample were acquired. The low-noise spectra, acquired with the valves closed, were later averaged together (by sample) to further improve the signal-to-noise ratio. When flying down the long axis of the plume, at a constant altitude in the smoke, the valves were set to automatically open and close at preset intervals (usually 90-120 s closed, 30 s open). Because all the long axis sampling took place in the smoke, a background sample collected at the same altitude prior to the long axis sampling was used to analyze the data (see section 2.4).

The flight plan for each Alaskan wildfire generally had several parts. First, to characterize the column just above the smoke source, pairs of "plume penetration" and background air samples were collected at several altitudes. Next, after moving 10-12 km downwind, background air samples and "cross-section" smoke samples were collected as we traversed the smoke plume at several altitudes. Then, if the wind direction and the surrounding terrain allowed, we would return to the origin of the plume and collect "long axis" smoke samples as we flew down the long axis of the plume at a constant altitude. Finally, if sufficient flight time remained, we completed another series of cross sections at the downwind end of the long axis flight.

2.3. Optical System

The AFTIR system was built to fit in a King Air B-90 aircraft along with a number of other smoke-sampling instruments. A detailed description of the AFTIR system, along with a schematic, is given by *Yokelson et al.* [1999]. A brief description follows. The system consisted of an infrared spectrometer operated at a resolution of 0.5 cm^{-1} (MIDAC Inc.), a White cell (IR Analysis, Inc.), and optical components mounted on a honeycomb-core, 28×175×11 cm optical table (Newport, Inc.) that was shock mounted (Aeroflex, Inc.) to the floor of the aircraft. To reduce spectral noise, rubber layers isolated the metal components of the shock mounts. The infrared beam exiting the spectrometer was directed by transfer optics to the "tripled" white cell. The beam made 120 passes of the 0.81 m basepath cell for a total path length of 97.5 m. After exiting the cell the infrared beam was directed by another set of transfer optics through a 25 mm focal length ZnSe lens and onto a LN_2-cooled, "midband" IR detector (Graseby, Inc., model FTIR M-16). Air pressure within the cell was measured by a capacitive transducer (Setra, Inc.) and recorded every second. Two thermocouples mounted at each end of the cell measured the cell temperature, which was also recorded every second.

2.4. Mixing Ratio Retrievals and Accuracy

A typical flight produced almost 5000 "raw" FTIR spectra (collected every 1.7 s). Selected raw spectra were coadded, as discussed earlier, to form high-quality "sample" spectra of background air and smoke. Mixing ratios for H_2O, CO_2, CO, CH_4, NO, C_2H_2, HCN, and HCHO were obtained by fitting sections of the single-beam transmission sample spectra with synthetic calibration classical least squares methods described fully elsewhere [*Griffith*, 1996; *Yokelson et al.*, 1996a, 1996b, 1997]. Absorbance, smoke sample spectra were generated by using background sample spectra collected at the same altitude and they were analyzed by spectral subtraction [*Yokelson et al.*, 1997] to yield mixing ratios for H_2O, HCOOH, CH_3COOH, NH_3, C_2H_4, CH_3OH, and O_3. (Our analysis for HCOOH by spectral subtraction properly treats the overlapping HDO lines [*Perrin et al.*, 1999].) We developed software to efficiently perform both types of mixing ratio retrievals for large numbers of spectra acquired at many different temperatures and pressures. The detection limits varied from spectrum to spectrum depending on the amount of water, the amount of signal averaging, fluctuation in spectrometer performance, and the analysis method. For most compounds the detection limit was usually 5-10 ppbv, but for HCHO it was usually 15-20 ppbv and for NO, under the conditions of this experiment, it was about 50 ppbv. The typical uncertainty in the excess mixing ratios in this work is

estimated to be ± 5% (1σ), or the detection limit, whichever is larger.

We investigated the stability of concentrated smoke samples (~50 ppm CO) that were stored in our cell (in the dark) for up to 24 hours (or in stainless steel canisters for ~4 hours). In these laboratory tests, CO_2, CO, CH_4, and C_2H_4 were stable, but many of the other species we report decreased significantly in < 1 hour. Thus we carefully examined our airborne grab samples of smoke at high time resolution. At the lower concentrations encountered in the field, NH_3 was the only compound for which the mixing ratios changed during the few minutes that the smoke samples were stored in the cell. The NH_3 decayed with a $1/e$ lifetime of ~35 s that is consistent with a first-order wall loss as shown by *Yokelson et al.* [1999]. Thus a modified analysis procedure was used for NH_3 in which the raw smoke spectra were analyzed at higher time resolution and the resulting mixing ratios were then back corrected to "time zero," assuming a first-order decay.

2.5. Auxiliary Measurements

In addition to the AFTIR system, the King Air also carried instrumentation that measured CO_2 and H_2O (Licor model Li6262), CO (TECO model 48), smoke absorption (Radiance Research), and particle light scattering (Radiance Research Nephelometer M903). Data from each of these instruments and our Global Positioning System (Magnavox) were recorded every second. Smoke samples were also collected in stainless steel canisters and in a 0.3 m^3 Tedlar bag (~ 6 s fill time). Particles were sampled on Teflon filters collected from smoke in the Tedlar bag or ambient air. The bag was also occasionally used as a source for canister samples or the real-time instruments. The stainless steel canister samples were later analyzed for CO_2, CO, and hydrocarbons using a gas chromatograph with a flame ionization detector. The measurements of trace gases and particulate matter by these instruments will be reported separately.

We employed a Cessna 172 fitted with a meteorological sonde (Aventech, Inc.) during the second half of our field campaign in Alaska. This aircraft was used to fly vertical profiles upwind and downwind of the fires collecting data on the air temperature, dew point, RH, air pressure, wind speed, wind direction, latitude, longitude, and altitude.

3. Results and Discussion

In the AFTIR spectra acquired in this study we were able to locate features due to H_2O, O_3, CO_2, CO, CH_4, C_2H_4, C_2H_2, HCHO, CH_3OH, HCOOH, CH_3COOH, NO, NH_3, and HCN. Thus these compounds were 14 of the most abundant compounds in the smoke (for reasons explained in section 2.1. of *Goode et al.* [1999]). Based on the analysis of the "smoke" and "background" sample spectra, we report excess mixing ratios for the compounds detected in the individual smoke samples collected < 18 km from the source of fires B320, B280, B349, and B309 in Tables 1-4, respectively. The local time and the altitude (above ground level) of each measurement are also shown. The sample names relate to the description of the flight plans (section 2.2): PP, plume penetration sample; XC, cross section sample; LAX, long axis sample. The samples collected >27 km downwind are discussed separately in section 3.4.

Table 1. Excess Mixing Ratios for All the Compounds Detected in the AFTIR Spectra Acquired Near the Source of Fire B320 on June 13, 1997[a]

Sample	Altitude,[b] m (AGL)	Time[c]	CO_2	CO	NO	CH_4	HCHO	NH_3	CH_3OH	HCOOH	CH_3COOH	C_2H_4	C_2H_2	HCN
PP1	105	14:39	33.5	1.82	0.069	0.182	0.041	0.026	0.018	0.020	0.038	0.078	0.020	
PP2	148	14:51	76.9	6.27	0.141	0.394	0.175	0.097	0.095	0.070	0.097	0.243	0.070	0.047
PP3	165	15:05	27.2	2.42		0.188	0.063	0.041	0.037	0.032	0.042	0.100	0.030	
PP4			47.0	4.22	0.108	0.320	0.101	0.052	0.071	0.052	0.064	0.152	0.045	0.024
									Intercompound Ratios					
				CO/CO_2	NO/CO_2	CH_4/CO	HCHO/CO	NH_3/CO	CH_3OH/CO	HCO_2H/CO	CH_3CO_2H/CO	C_2H_4/CO	C_2H_2/CO	HCN/CO
Emission ratio calculated from slope				0.0808	0.0020	0.0695	0.0264	0.0147	0.0153	0.0116	0.0158	0.0384	0.0112	0.0069
R^2				0.91	0.87	0.82	0.98	0.95	0.96	0.97	0.95	0.99	0.99	0.84
			CO_2	CO	NO	CH_4	HCHO	NH_3	CH_3OH	HCOOH	CH_3COOH	C_2H_4	C_2H_2	HCN
Emission factors, g kg^{-1}			1664	85.5	2.27	3.45	2.38	0.77	1.45	1.57	2.95	3.28	0.88	0.61
Modified combustion efficiency			0.925											
Combustion efficiency			0.908											

[a]Mixing ratios in units Δppmv. AGL, above ground level.
[b]To convert to altitude above mean sea level (MSL), add 450 m.
[c]Local Alaskan time is reported.

Table 2. Excess Mixing Ratios for All the Compounds Detected in the AFTIR Spectra Acquired Near the Source of Fire B280 on June 21, 23, and 24, 1997[a]

Sample	Altitude,[b] m (AGL)	Time[c]	CO_2	CO	CH_4	HCHO	NH_3	CH_3OH	HCOOH	CH_3COOH	C_2H_4	C_2H_2
						June 21, 1997						
PP1	278	19:16	10.6	1.30	0.085	...	0.021	...	...	0.022	0.039	...
PP2	155	19:27	19.3	1.86	0.119	...	0.051	...	...	0.016	0.067	...
PP3	39	19:37	23.3	1.84	0.149	0.038	0.058	0.018	...	0.016	0.065	...
XC1 2500	554	19:57	15.2	0.96	0.109	...	...	...	...	...	0.035	...
XC1 3500	981	20:00	17.3	1.11	0.123	...	0.030	0.012	...	...	0.045	...
LAX1-1	1065	20:12	23.9	1.69	0.153	...	0.027	...	...	0.018	0.049	...
LAX1-2	1002	20:13	12.7	1.02	0.101	...	0.057	...	...	0.018	0.027	...
LAX1-3	956	20:14	17.6	1.07	0.123	...	0.039	...	...	...	0.035	...
PP4	188	20:40	32.6	3.03	0.186	...	0.072	0.050	...	0.036	0.066	...
						June 23, 1997						
PP1	599	16:53	16.0	1.35	0.071	...	0.054	0.011	...	0.032	0.052	...
PP2	472	16:56	32.3	2.02	0.106	0.047	0.049	0.027	...	0.041	0.077	...
PP3	413	17:07	67.6	7.18	0.412	0.133	0.187	0.102	0.038	0.120	0.150	0.019
XC1 1000	676	17:18	16.3	1.54	0.089	...	0.030	0.024	...	0.034	0.053	...
XC1 2000	1006	17:23	12.0	1.85	0.111	...	0.033	0.023	...	0.041	0.050	...
XC1 3000	1224	17:28	31.4	3.01	0.210	...	0.068	0.042	0.024	0.063	0.085	...
XC1 4000	1544	17:34	26.3	2.89		0.082	0.042	0.037	0.020	0.045	0.055	...
LAX1-1	1408	18:01	52.1	4.24	0.192	0.094	0.052	0.044	0.020	0.060	0.110	0.012
LAX1-2	1406	18:03	25.6	2.67	0.123	0.060	0.034	0.029	0.023	0.053	0.072	
						June 24, 1997						
PP1	615	14:12	21.70	1.74	0.137	...	0.026	0.025	...	0.036	0.036	...
PP2	382	14:26	9.07	1.32	0.085	...	0.036		...	0.026	0.029	...

	Intercompound Ratios								
	CO/CO_2	CH_4/CO	HCHO/CO	NH_3/CO	CH_3OH/CO	HCO_2H/CO	CH_3CO_2H/CO	C_2H_4/CO	C_2H_2/CO
Emission ratio calculated from slope	0.0917	0.0601	0.0207	0.0257[d]	0.0132	0.0058	0.0165	0.0249	0.0027
R^2	0.89	0.78	0.86	0.95	0.93	0.35	0.86	0.76	0.99

	CO_2	CO	CH_4	HCHO	NH_3	CH_3OH	HCOOH	CH_3COOH	C_2H_4	C_2H_2
Emission factors, g kg^{-1}	1653	96.5	3.31	2.25	1.49	1.44	1.04	3.38	2.42	0.29
Modified combustion efficiency	0.916									
Combustion efficiency	0.902									

[a]Mixing ratios in units Δppmv. AGL, above ground level.

[b]To convert to altitude above mean sea level (MSL), add 450 m.

[c]Local Alaskan time is reported.

[d]Calculated using only the plume penetration samples. Changing to this procedure did not significantly affect any other source estimate.

Table 3. Excess Mixing Ratios for All the Compounds Detected in the AFTIR Spectra Acquired Near the Source of Fire B349 on June 22, 1997[a]

Sample	Altitude,[b] m (AGL)	Time[c]	CO_2	CO	NO	CH_4	HCHO	NH_3	CH_3OH	HCOOH	CH_3COOH	C_2H_4	C_2H_2
PP1	89	15:10	92.1	7.32	0.182	0.389	0.116	0.113	0.126	0.028	0.077	0.099	0.022
PP2	140	15:18	108.5	6.86	0.148	0.326	0.112	0.061	0.088	0.044	0.047	0.101	0.020
PP3	129	15:23	204.2	15.47	0.262	0.717	0.266	0.185	0.189	0.077	0.141	0.210	0.042
PP4	278	15:35	46.7	3.02	0.079	0.192	0.059	0.022	0.046	0.021	0.027	0.046	0.011
XC1 2500	883	15:50	64.5	5.56	0.093	0.316	0.107	0.073	0.072	0.023	0.039	0.094	0.014
XC1 3500	1090	15:53	72.7	6.53	0.125	0.287	0.120	0.089	0.089	0.044	0.051	0.092	0.015
PP6	82	16:19	29.4	3.64		0.253		0.045	0.062	0.022	0.021	0.038	0.010

	Intercompound Ratios									
	CO/CO_2	NO/CO_2	CH_4/CO	HCHO/CO	NH_3/CO	CH_3OH/CO	HCO_2H/CO	CH_3CO_2H/CO	C_2H_4/CO	C_2H_2/CO
Emission ratio calculated from slope	0.0760	0.0014	0.0489	0.0172	0.0122	0.0133	0.0052	0.0087	0.0139	0.0028
R^2	0.94	0.82	0.92	0.99	0.92	0.90	0.85	0.94	0.97	0.97

	CO_2	CO	NO	CH_4	HCHO	NH_3	CH_3OH	HCOOH	CH_3COOH	C_2H_4	C_2H_2
Emission factors, g kg^{-1}	1688	81.6	1.61	2.27	1.50	0.59	1.23	0.71	1.61	1.18	0.20
Modified combustion efficiency	0.929										
Combustion efficiency	0.920										

[a]Mixing ratios in units Δppmv. AGL, above ground level.

[b]To convert to altitude above mean sea level (MSL), add 450 m.

[c]Local Alaskan time is reported.

Table 4. Excess Mixing Ratios for All the Compounds Detected in the AFTIR Spectra Acquired Near the Source of Fire B309 on June 24 and 27, 1997[a]

Sample	Altitude,[b] m (AGL)	Time[c]	CO_2	CO	NO	CH_4	HCHO	NH_3	CH_3OH	HCOOH	CH_3COOH	C_2H_4	C_2H_2
							June 24, 1997						
PP3	655	15:00	80.2	7.33	0.101	0.424	0.127	0.089	0.117	0.055	0.079	0.137	0.018
XC1 4000	1598	15:15	9.4	1.13	...	...	0.040	...	...	0.018	0.018	0.029	...
XC1 6000	2085	15:20	26.2	2.41	0.050	0.106	0.055	0.043	·0.025	0.021	0.039	0.046	...
LAX1-1	1330	15:41	14.2	1.38	...	0.142	...	0.026	...	0.016	0.027	0.039	...
							June 27, 1997						
PP1	473	16:53	49.8	4.40	...	0.182	0.072	0.043	0.041	0.031	0.048	0.077	0.012
XC1 1000	601	17:02	11.6	1.12	...	0.101	...	0.018	...	...	0.015	0.025	...
XC1 3500	1229	17:10	14.7	1.28	...	...	...	0.013	...	...	0.019	0.023	...

	Intercompound Ratios									
	CO/CO_2	NO/CO_2	CH_4/CO	HCHO/CO	NH_3/CO	CH_3OH/CO	HCO_2H/CO	CH_3CO_2H/CO	C_2H_4/CO	C_2H_2/CO
Emission ratio calculated from slope	0.0910	0.0013	0.0545	0.0178	0.0122	0.0140	0.0077	0.0115	0.0188	0.0025
R^2	1.00	0.80	0.85	0.87	0.89	0.85	0.87	0.89	0.97	0.83

	CO_2	CO	NO	CH_4	HCHO	NH_3	CH_3OH	HCOOH	CH_3COOH	C_2H_4	C_2H_2
Emission factors, g kg^{-1}	1659	96.1	1.47	2.96	1.81	0.70	1.57	1.21	2.26	1.79	0.20
Modified combustion efficiency	0.917										
Combustion efficiency	0.905										

[a]Mixing ratios in units Δppmv. AGL, above ground level.
[b]To convert to altitude above mean sea level (MSL), add 450 m.
[c]Local Alaskan time is reported.

3.1. Estimation of Fire-Average Emission Ratios and Emission Factors

We estimate fire-average emission ratios, between compounds, from the slope of the least squares line, with the intercept forced to zero, in a plot of one set of excess mixing ratios versus the other. This procedure is justified in detail by *Yokelson et al.* [1999] and *Little and Rubin* [1987]. Figure 2 shows these emission ratio plots for all the compounds detected, except HCN and O_3. The excess mixing ratios of each compound have been plotted against the excess mixing ratios of CO, except for NO, which was plotted against CO_2 since they are both "flaming compounds," and CO, which was plotted against CO_2 to examine the efficiency of the

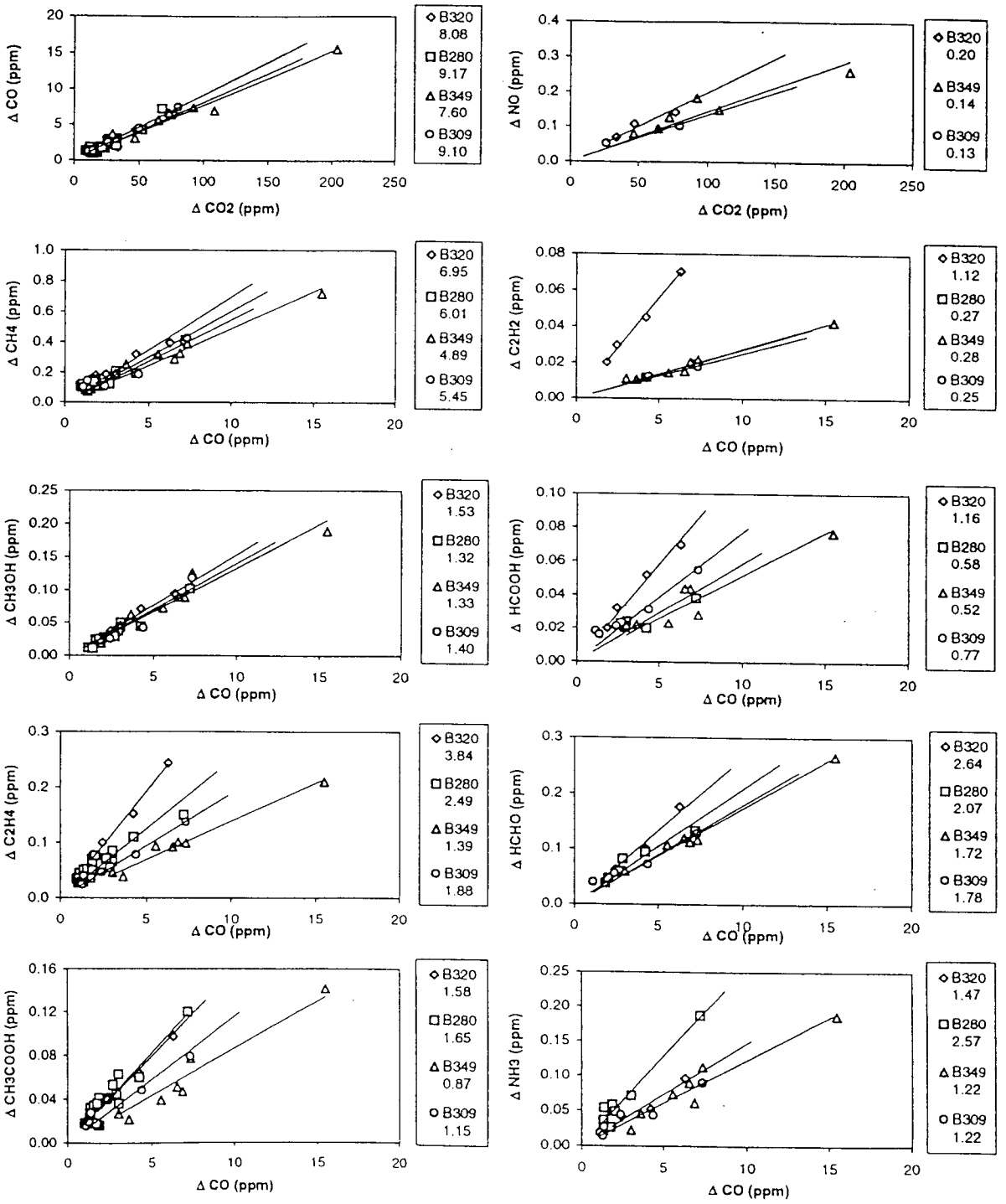

Figure 2. The excess mixing ratios measured near the source for selected compounds plotted against either excess CO_2 or excess CO. In the plot for each compound, data from each of the four fires are indicated by the symbol specified in the legend. The emission ratio derived from the slope of the linear regression line is shown as a percent for each fire under its label in the legend and in Tables 1-4 (where the R^2 values for each regression line can also be found).

combustion [*Yokelson et al.*, 1996b]. We report these fire-average emission ratios in Tables 1-4. Fires B280 and B309 were both sampled on several different days, and the fire-average emission ratios displayed in Figure 2 and given in the tables are derived from all the source data for the fires. (No significant variations were observed between the individual, daily, fire-average emission ratios, and the fires were noted to be burning in a similar mixture of fuels each day.) In Table 5 we compare our fire-average emission ratios with those from other laboratory and field investigations. For almost all the compounds we measured in this study, the fire-average emission ratios were within, or near, the range of previous measurements. An exception to this is the C_2H_4/CO emission ratio for which half of our Alaska measurements are larger than those measured previously.

We report estimated, fire-average emission factors in Tables 1-4 for each observed trace gas that are calculated from our fire-average emission ratios using the carbon mass balance method [*Ward and Radke*, 1993]. Our method of implementing the carbon mass balance method for airborne measurements was described in full by *Yokelson et al.* [1999]. In brief we assume that all the volatilized carbon is detected and that the fuel is 50% carbon by mass [*Susott et al.*, 1996]. By ignoring particulate and unmeasured gases we are probably inflating the emission factors by 1-2% and the actual fuel carbon percentage may vary by ± 10% (2σ). The fire-average modified combustion efficiency (MCE) and the fire-average combustion efficiency (CE) for the four wildfires are also given in Tables 1-4. Modified combustion efficiency is defined as $\Delta CO_2/(\Delta CO_2+\Delta CO)$; where the Δ indicates an excess mixing ratio [*Ward and Radke*, 1993]. The table MCE values have been calculated using the $\Delta CO/\Delta CO_2$ emission ratio and the equation $MCE = 1/((\Delta CO/\Delta CO_2)+1)$. CE, the fraction of burned carbon released as CO_2, was estimated from the molar ratio of CO_2 to total measured carbon. CE and MCE are useful as indexes of the relative amount of flaming and smoldering combustion throughout a fire, and MCE is used to compare studies in sections 3.2 and 3.3.

In this study it was only possible to sample smoke plumes during the afternoon and early evening, which is when the fuel consumption rate is often the highest. Airborne and ground-based sampling have been directly compared, on the same fire, on two occasions. *Susott et al.* [1991] reported a ground-based value for the fire-average CO emission factor that was 10% higher than the airborne value [*Radke et al.*, 1991] for a summer, boreal forest fire. *Ward et al.* [1992] reported a ground-based value for the fire-average CO emission factor that was 37% higher than the airborne value for an autumn fire in a moist temperate forest. Thus our fire-average emission ratios and emission factors may be reasonably representative of the fire-average emissions for midseason burning conditions. In addition, it is important to note that if our measurements did oversample flaming or smoldering combustion, the relationships obtained between MCE and the emission factors should still be valid.

3.2. Initial Emissions of Oxygenated Organic Compounds From Biomass Fires

Oxygenated organic compounds are important as HO_x sources in the global-regional troposphere and in smoke plumes [*Finlayson-Pitts and Pitts*, 1986; *Griffith et al.*, 1991; *Singh et al.*, 1995; *Yokelson et al.*, 1996b, 1999; *Wennberg et al.*, 1998]. *Yokelson et al.* [1996b] reported emission factors measured by open-path FTIR (OP-FTIR) for a variety of oxygenated organic compounds released by laboratory fires that burned in softwood and sagebrush fuels at various MCEs. They concluded that fires were a significant, but previously underestimated, source of these compounds. For example, the sum of the three main oxygenated organic emissions (formaldehyde, methanol, and acetic acid) was comparable to the methane emissions. Three subsequent laboratory OP-FTIR studies confirmed similar, large emissions of oxygenated organic compounds from fires in grass, hardwood, organic soil, and softwood fuels [*Yokelson et al.*, 1997, 1998; *Goode et al.*, 1999]. Our first airborne FTIR (AFTIR) measurements of fire emissions of oxygenated organic compounds (in North Carolina) agreed very well with our extensive, OP-FTIR, laboratory fire emissions data for these compounds [*Yokelson et al.*, 1999]. This result provided additional evidence of the importance of fires as a source of these compounds (and also suggested a strong similarity between the emissions from our laboratory fires and the emissions from full-scale field fires). However, in the North Carolina study we measured emission factors for only two fires. Our AFTIR measurements from Alaska provide emission factors for four more fires, probe new fuels, and allow more comprehensive conclusions from our accumulated work as discussed next.

We plot the emission factors for the three oxygenated organic compounds that are produced most abundantly by fires (formaldehyde, methanol, and acetic acid) versus fire MCE in Figures 3a-3c. The graphs include the fire emission factors from our AFTIR field measurements in Alaska and North Carolina; our laboratory, OP-FTIR measurements for aboveground biomass; and emission factors published before our FTIR-based studies by other groups that used a variety of other techniques. For each compound we derive a regression line based on all the emission factors from the AFTIR studies and the laboratory, OP-FTIR studies of aboveground biomass [*Yokelson et al.*, 1996b, 1997, 1998, 1999; *Goode et al.*, 1999; this work], but excluding emission factors from the earlier work. With these restrictions, a single, highly correlated, linear model fits the data for each of these three compounds. It is clear that both the Alaska and North Carolina field data lie very close to the line established primarily by our laboratory data. It is also clear that the data from the other studies show little or no linear correlation with MCE and significantly lower absolute values.

Taken together these results have a number of important implications. (1) The Alaska results provide significant, additional confirmation that the emissions from real fires can be similar to the emissions from our carefully modeled laboratory fires. (2) The linear relationships derived in Figures 3a-3c fit data from fires in a wide variety of locations and fuels (now including boreal zone fuels in Alaska). This suggests that the plots are useful as simple models to predict the emissions of HCHO, CH_3OH, and CH_3COOH from fires for which these compounds have not been explicitly measured. This is true as long as the CO and CO_2 emissions have been measured or can be estimated. Similar plots can be constructed for formic acid, phenol, and hydroxyacetaldehyde using the data in Tables 1-4 and the references. (3) There is a wide range in emission factors as a function of MCE. For example, we predicted that the emission factors for oxygenated compounds would be considerably higher for tropical deforestation fires (MCE ~0.89) than for savanna fires (MCE ~0.94) [*Yokelson et al.*, 1999]. (4) Fires are again confirmed as an important source of

Table 5. Selected Data From *Nance et al*. [1993] and the Published Studies That Included Measurements of the Initial Emissions of the Major Oxygenated Organic Compounds From Biomass Fires[a]

			Emissions as % of CO_2	Emissions as % of CO													
				Hydrocarbons					Aldehydes		Acids		Alcohols		Nitrogen[b]		Sulfur
Study	Method	L/F[c]	NO	CH_4	C_2H_6	C_2H_4	C_2H_2	C_3H_6	HCHO	Glycol-	Formic	Acetic	CH_3OH	C_6H_6O	NH_3	HCN	OCS
Griffith et al. [1991]	OP-FTIR	F	0.095	7.61	...	...	...	...	1.27	...	...	...	...	...	3.24	0.12	...
Yokelson et al. [1996b]	OP-FTIR	L	0.178	10.9	1.42	1.71	0.98	...	1.6	...	0.73	2.32	1.61	...	1.91	0.44	...
Yokelson et al. [1997]	OP-FTIR	L	...	6.55	0.45	0.98	0.17	0.65	2.33	1.08	1.09	2.2	1.98	0.84	2.66	0.65	0.04
Yokelson et al. [1998]	OP-FTIR	L	0.128	6.43	...	1.49	...	...	1.55	...	0.58	1.12	1.21	...	1.42	...	...
Goode et al. [1999]	OP-FTIR	L	0.145	8.06	...	1.97	0.37	1.14	1.8	0.51	1.12	1.47	1.21	...	1.31	...	...
Yokelson et al. [1999] CL1	AFTIR	F	...	7.7	...	...	...	...	2.6	...	...	...	...	...	...	...	...
Yokelson et al. [1999] WF1	AFTIR	F	...	...	...	1.4	...	...	3.3	...	1.2	1.6	2.4	...	2.6	...	...
Yokelson et al. [1999] CL2	AFTIR	F	...	11.4	...	1.5	...	...	2.6	...	0.85	1.8	2.1	...	1.1	...	...
Alaskan wildfire B320	AFTIR	F	0.20	6.95	...	3.84	1.12	...	2.64	...	1.16	1.58	1.53	...	1.47	0.69	...
Alaskan wildfire B280	AFTIR	F	...	6.01	...	2.49	0.27	...	2.07	...	0.58	1.65	1.32	...	2.57	...	...
Alaskan wildfire B349	AFTIR	F	0.14	4.89	...	1.39	0.28	...	1.72	...	0.52	0.87	1.33	...	1.22	...	...
Alaskan wildfire B309	AFTIR	F	0.13	5.45	...	1.88	0.25	...	1.78	...	0.77	1.15	1.40	...	1.22	...	...
Talbot et al. [1988]	MIST	L	...	...	...	...	...	...	...	...	0.009	0.09	...	...	...	...	...
Nance et al. [1993]	GC/MS/EC	F	...	5.7	0.73	...	0.35	0.42	...	...	...	...	...	...	1.3	...	...
McKenzie et al. [1995]	GC/MS	L	...	2.9	0.25	1.2	...	...	...	...	0.15	0.74	1.1	0.03	...	...	...
Worden et al. [1997]	AES	F	...	...	...	...	...	...	...	...	1.55	...	3.1	...	4.3	...	...
Hurst et al. [1994]	MI-FTIR	F	...	4.5	...	...	0.07	...	0.25	...	...	...	...	...	2.6	0.03	...
Holzinger et al. [1999]	CIMS	L	...	...	...	...	...	...	2.21	...	...	...	0.64	...	...	0.12	...
Average of above	All		0.145	6.79	0.71	1.80	0.43	0.74	1.98	0.80	0.79	1.38	1.61	0.44	2.07	0.34	0.04

[a]The study means are reported expressed as molar percentages of CO_2 or CO. The value of one standard deviation is typically from 1/3 to 2/3 of the mean. Three dots indicate that the compound was below the detection limits or it was not measured. Abbreviations are OP-FTIR, open-path Fourier transform infrared spectroscopy; MIST, mist chamber (see reference); GC, gas chromatography; MS, mass spectrometry; EC, electron capture; AES, airborne emission spectrometer (operates in the infrared region); MI-FTIR, matrix isolation FTIR; CIMS, chemical ionization mass spectrometer.

[b]Highly dependent on fuel nitrogen content.

[c]Fire location: L, laboratory; F, field.

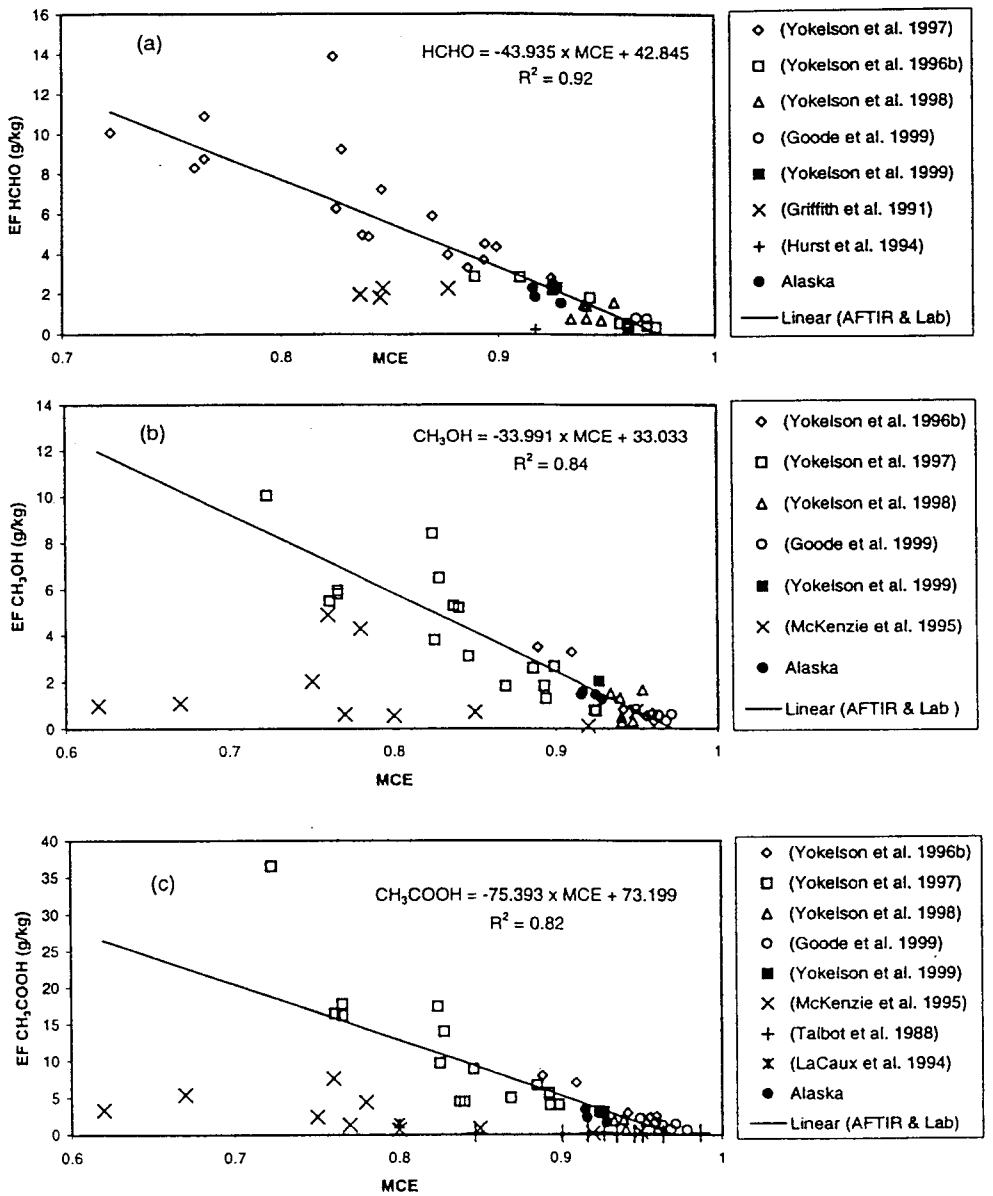

Figure 3. Emission factors (EF, g kg^{-1} dry fuel) plotted against MCE for (a) formaldehyde, (b) methanol, and (c) acetic acid. The linear regression line was fit using all the AFTIR field results and the OP-FTIR laboratory results, but excluding other results. The field data from Alaska and North Carolina are both close to the "best fit" line for each compound. The linear regression fits shown are useful for estimating emissions of these compounds as discussed in section 3.2.

oxygenated organic compounds (which may have been previously underestimated). For instance, *Yokelson et al.* [1999] calculated that fires account for 10-30% of the global tropospheric methanol source.

3.3. Initial Emissions of Reactive Nitrogen Compounds

Biomass burning is an important source of reactive nitrogen in the atmosphere. NH_3, NO_x, and N_2, which is not readily measurable by IR spectroscopy, account for most of the fuel nitrogen volatilized by biomass burning [*Goode et al.*, 1999]. The nitrogen-containing emissions measured in this study were NO from flaming combustion and NH_3 and HCN from smoldering combustion. Other nitrogen-containing compounds such as NO_2 and N_2O were below our detection limits. The average NH_3/CO molar emission ratio for our Alaskan wildfires (1.6%) is a little below the average of the NH_3/CO emission ratios shown in Table 5 (~2%), but within the range of measured values, including that of *Nance et al.* [1993] who reported an NH_3/CO emission ratio of 1.3% for an early July Alaskan fire. These observations are consistent with high-latitude, aboveground vegetation being low in nitrogen content [*Chapin and Shaver*, 1985]. This may also indicate that little consumption of the organic soil layer occurred during these studies since *Yokelson et al.* [1997] measured an average NH_3/CO emission ratio of ~5% for smoldering, Alaskan organic soils. In *Yokelson et al.* [1996b] we plotted the published measurements of the molar emission ratio NH_3/NO_x versus MCE and used linear regression to obtain the equation NH_3/NO_x = (-14.0 × MCE) + 13.8 (r^2=0.96). This result confirmed that NO_x (primarily NO) is the dominant

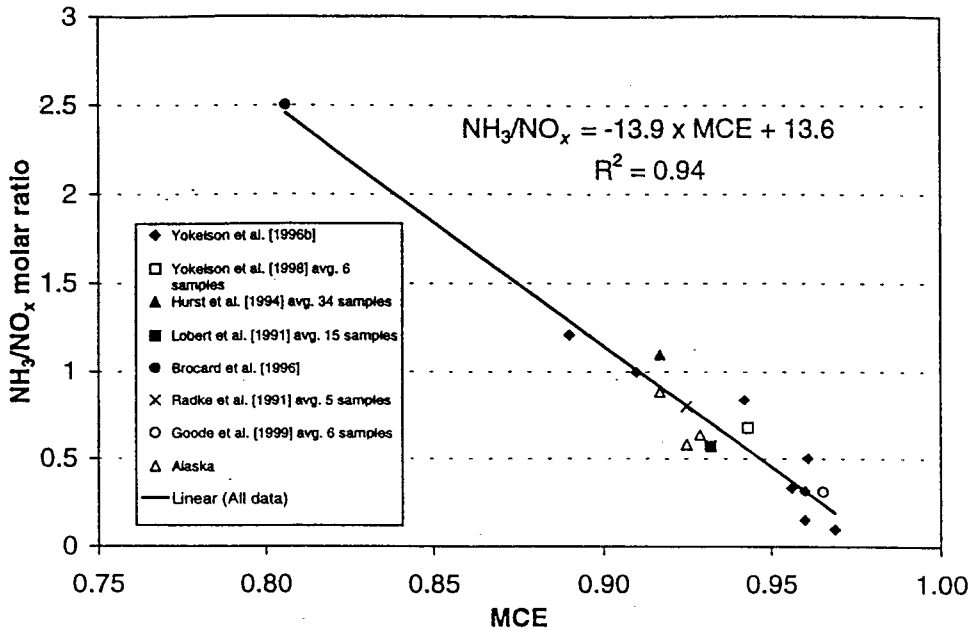

Figure 4. The fire-average NH_3/NO_x molar emission ratio plotted versus the fire-average MCE. The values for the Alaska wildfires are shown with the other published measurements of this ratio, which were reported in studies carried out in a variety of tropical and temperate fuels. The linear regression fit shown is useful for estimating emissions of these compounds as discussed in section 3.3.

reactive nitrogen emission from flaming combustion, and NH_3 is the main reactive nitrogen emission from smoldering combustion. In Figure 4 we again plot NH_3/NO_x as a function of MCE but now include data from our more recent laboratory studies and the Alaska wildfires. The Alaska data lie very near the new linear regression line (based on all the data), which has nearly the same equation: NH_3/NO_x = (-13.9 × MCE) + 13.6 (r^2=0.94). Thus this simple, linear model fits data from a wide variety of independent fire measurements in tropical to boreal zone fuels. The linear equation can be used to estimate the emissions of one compound when measurements were only made of the other. Since NH_3+NO_x usually accounts for 25 - 50% of the fuel nitrogen [*Goode et al.*, 1999] and nitrogen content is available for many fuels [*Susott et al.*, 1996], the equation can also be used to estimate production of both compounds when neither was measured.

3.4. Chemical Transformations in the Nascent Plume

Many of the trace gases emitted by fires are too reactive to become well mixed in the global troposphere. Photochemical reactions and other processes consume many of the initial emissions and produce new species. Much of this change occurs at chemical and particle concentrations well outside the "normal" range. Thus the details of these transformations are not well understood, but they should depend strongly on the mix of initial emissions and the changing physical state of the plume. CO has a lifetime of 1 to 6 months in the troposphere, and CO is the major smoke component that is least abundant in background air. Although CO is not a strictly conserved plume tracer, its mixing ratio does provide a good short-term indication of plume location and dilution rate. The photochemical oxidation of CO in the presence of NO_x produces O_3. Thus the ratio $\Delta O_3/\Delta CO$ is used as an indicator of the degree of photochemical aging in biomass burning plumes in many experimental [*Andreae et al.*, 1988, 1994; *Lindesay et al.*, 1996] and modeling studies [*Chatfield and Delaney*, 1990; *Fishman et al.*, 1991; *Jacob et al.*, 1992, 1996; *Chatfield et al.*, 1996; *Lelieveld et al.*, 1997; *Mauzerall et al.*, 1998]. A range of $\Delta O_3/\Delta CO$ ratios have been measured in biomass-burning haze layers of various ages and initial $\Delta NO_x/\Delta CO$ ratios. In haze layers 1-2 days old, $\Delta O_3/\Delta CO$ ratios of 0.04 - 0.18 were measured during the Arctic Boundary Layer Expedition (ABLE 3A) study over Alaska [*Wofsy et al.*, 1992] and ratios of 0.1 - 0.2 were measured during the ABLE 3B study over eastern Canada [*Mauzerall et al.*, 1996]. High ratios, up to 0.88, were measured at the top of haze layers that had aged about 10 days in the tropics [*Andreae et al.*, 1994]. In many studies the haze layers contain the products of many fires burning over a wide area, making assignment of a single, narrowly defined, chronological smoke "age" difficult or even irrelevant. In contrast, *Stith et al.* [1981] used an O_3-C_2H_4 chemiluminescence instrument to map out ozone mixing ratios in an isolated, fresh, biomass-burning plume. At the source, or near the bottom of the (horizontally drifting) plume, they measured very low or negative ΔO_3 values, which they attributed to titration by NO and low UV intensity. Near the top of the plume, 10 km downwind and in smoke < 1 hour old, they measured ΔO_3 values as high as 44 ppbv. High ΔO_3 was positively correlated with high UV.

One of the goals of our Alaska study was to use the broadband detection capacity of AFTIR to probe the rate of chemical transformations in isolated biomass burning plumes where a narrowly defined smoke age would be both relevant and measurable. Conditions allowing this type of downwind sampling occurred on June 23 at fire B280 and on June 27 at fire B309, both in the early evening. Both of these fires generated large, lofted smoke plumes that extended ~100 km downwind. Measurements with the airborne sonde on June 23 at ~1730 LT showed that the wind speed within the smoke plume was 5.5 ± 1.5 m s^{-1}. On June 27 at ~1730 LT we

measured a constant wind speed below, within, and above the smoke plume of 7 ± 2 m s^{-1}. On both of these days, ground level wind speed data (from remote weather stations located near the fires) and balloon-borne wind measurements from the towns of McGrath and Galena (Figure 1) indicated that the early afternoon wind conditions were very similar to those that we measured during the late afternoon/early evening. Thus we assumed that the fire emissions were transported at a constant rate from the source to the sampling point to calculate the age of the downwind smoke samples shown in Table 6.

On the June 27 flight, smoke samples were collected from the top ~50 m of the plume and the smoke spectra showed prominent ozone features. Analysis of these features revealed that the O_3 formation rate in the upper, early plume was ~50 ppbv hr^{-1}. In addition, $\Delta O_3/\Delta CO$ ratios of 0.04 - 0.089 (~10% of the maximum observed values in these plumes) were reached within only ~2 hours (Table 6). In contrast, on the June 23 flight, smoke samples were collected approximately 300 m below the top of the smoke plume and no ozone spectral features were seen (detection limit of ~20 ppbv) (Table 6). This result was probably due to reduced UV since the percentage of high cloud cover was a little larger on June 23 and, well inside the plume, absorption of UV light by smoke particles could decrease photolysis rates. (Nephelometer data from the two flights indicate that 350-600 μm^{-3} of particulate matter were present in both downwind smoke plumes.) We note that measurements in power plant plumes also show early O_3 production occurring at the edges of the plume [*Senff et al.*, 1998]. The different O_3 production between flights could also be due to a different NO/CO emission ratio for the two fires. Our "raw" concentration retrievals yielded similar NO/CO emission ratios for fires B280 and B309, but the NO mixing ratios for the less-concentrated B280 plume were all near, or below, our detection limit, so we cannot confidently report a NO/CO emission ratio for this fire.

An interesting downwind chemical transformation was clearly measured in our June 23 central plume samples (for which no O_3 production was observed). From Table 6 it is clear that the $\Delta NH_3/\Delta CO$ ratio on this fire (B280) decreased consistently with time downwind and decayed to 1/*e* of its initial value in ~2.5 hours. This loss rate is consistent with the observations of *Andreae et al.* [1988]. They measured particle-NH_4^+/CO_g ratios of 0.7 - 1.5 in "fresh" biomass burning plumes possibly due to rapid conversion of gas phase NH_3 to particle NH_4^+.

On the June 27 flight both $\Delta HCOOH/\Delta CO$ and $\Delta CH_3COOH/\Delta CO$ were ~2 times higher in the downwind samples. On the June 23 flight formic acid showed a similar increase, but acetic acid appeared to increase and then decrease (Table 6). Secondary sources of formic acid relevant to polluted air have been described [*Finlayson-Pitts and Pitts*, 1986, pp. 394 and 454] and *Jacob et al.* [1992, 1996] discussed several gas phase sources of acetic acid that could occur in biomass burning plumes. Our initial experiments may indicate the approximate timescale of organic acid production in actual plumes. Not only do our current data tentatively confirm a rapid secondary source of organic acids in the plume, but our studies have consistently indicated that the organic acid emission factors for fires are larger than was previously believed [*Yokelson et al.*, 1996b, 1997, 1998, 1999]. Both of these observations could help account for the "major unidentified source of atmospheric acetic acid" discussed by *Jacob et al.* [1992, pp. 16,421, 16,426, and 16,429] in their study of the high-latitude troposphere. In general, our first downwind observations still constitute a limited set of data. However, it seems likely that continued instrumental improvements and/or additional measurements will produce information useful for comparison to smoke chemistry models and as a link between source characterization and haze layer characterization experiments.

Earlier work at high latitudes indicated that fires contributed to O_3 levels mainly by increasing the regional NO_x, and slowing regional O_3 destruction, rather than in-plume production. This was primarily because rapid conversion of NO_x to reservoir species was observed and a low NO_x/CO emission ratio for boreal fires was proposed [*Bradshaw et al.*, 1991; *Singh*, 1991; *Jacob et al.*, 1992; *Singh et al.*, 1994; *Fan et al.*, 1994; *Mauzerall et al.*, 1996]. Our work confirms the low initial NO_x/CO emission ratio for boreal fires (1.6%, derived from Table 7) but also shows that rapid O_3 production can occur in portions of the early plume. An experiment similar to the one reported here but with extended downwind sampling could determine if significant, additional O_3 formation might sometimes occur within distinct plumes.

3.5. Annual Trace Gas Emissions From Fires in Alaska and the Global Boreal Forest

The fire-average emission ratios in Figure 2 and Tables 1-4 exhibit an interesting trend. For NO, CH_4, C_2H_2, CH_3OH, HCOOH, C_2H_4, and HCHO the highest fire-average emission ratios are all measured on wildfire B320. These higher emission ratios may be related to the fuels at this fire (low shrub and grassy vegetation), which were significantly different from the mixture of fuels for the other three wildfires. Several compounds exhibit very high fire-average emission ratios on fire B320. For example, the C_2H_2/CO emission ratio is almost four times higher for wildfire B320 (1.12%) than for the other Alaskan wildfires. If we omit the B320 result, the average C_2H_2/CO emission ratio for the other three Alaskan wildfires (0.27%) is reasonably close to the value of 0.35% measured by *Nance et al.* [1993] in their Alaskan wildfire study. The C_2H_4/CO fire-average emission ratio for fire B320 (3.84%) is significantly higher than the average of all the studies reported in Table 5 (1.80%). If we again omit the value for fire B320, then the fire-average emission ratio for the other three wildfires (1.92%) is very close to the average shown in Table 5.

The other three fires we studied burned in fuels more typical of Alaskan, boreal forest fires (spruce or spruce/bog/shrub mosaic). The Alaskan fire studied by *Nance et al.* [1993] burned in similar fuels and yielded similar emission results (see Table 5). Thus we derive a preliminary set of emission ratios and emission factors characteristic of Alaskan, boreal forest fires by combining results from the two studies. We take the arithmetic average of the emission ratios from our three boreal forest wildfires (B280, B349, and B309) and the emission ratios measured by *Nance et al.* [1993] to calculate the average, Alaskan, boreal forest fire emission ratios shown in Table 7. (The data from our grass and low shrub fire (B320) have not been included for the reasons given above.) In a similar manner we calculate average, Alaskan, boreal forest fire emission factors, which are also given in Table 7 along with emission factors for formaldehyde, methanol, and acetic acid predicted from the linear regression models shown in Figure 3 (using the boreal forest average MCE (0.923)). As expected, the model-predicted emission

Table 6. Excess Mixing Ratios, Ratio to Excess CO, and Sample Age for the Compounds Detected in AFTIR Spectra Acquired 28-56 km Downwind From the Source of Fire B280 or B309[a]

Sample	Altitude, m[b]	Time[c]	Distance, km	Age,[d] hours	CO emr	HCHO emr	HCHO %	NH_3 emr	NH_3 %	CH_3OH emr	CH_3OH %	HCOOH emr	HCOOH %	CH_3CO2H emr	CH_3CO2H %	C_2H_4 emr	C_2H_4 %	O_3 emr	O_3 %
Fire B280, June 23, 1997																			
Initial age and ratio to CO[e]				"0"			2.1		2.6		1.3		0.6		1.7		2.5		
Downwind																			
LAX1-3	1361	18:05	28	1.5 (0.4)	2.17	...	...	0.035	1.6	0.018	0.8	0.025	1.2	0.061	2.8	0.062	2.8	...	...
LAX1-4	1358	18:07	39	2.1 (0.6)	1.94	...	...	0.024	1.2	0.024	1.2	0.029	1.5	0.036	1.9	0.058	3.0	...	...
LAX1-5	1354	18:09	51	2.8 (0.8)	1.79	...	...	0.013	0.7	0.014	0.8	0.023	1.3	0.028	1.6	0.054	3.0	...	...
Fire B309, June 27, 1997																			
Initial age and ratio to CO[e]				"0"			1.8		1.2		1.4		0.8		1.2		1.9		
Downwind																			
LAX1-2	1852	17:34	39	1.7 (0.5)	1.22	...	...	...	...	...	...	...	...	0.029	2.4	0.022	1.8	0.109	8.9 ± 1.3
LAX1-3	1677	17:36	52	2.3 (0.6)	2.07	0.054	2.6	...	...	0.022	1.1	0.028	1.3	0.037	1.8	0.030	1.4	0.132	6.4 ± 0.9
XC2 5500	1752	17:50	56	2.4 (0.7)	1.20	...	...	...	...	...	...	0.020	1.6	0.034	2.8	0.020	1.6	0.101	8.4 ± 1.3

[a]Mixing ratios are in units Δppmv; ratios as a percentage. Data for CO_2 and CH_4 are omitted. Abbreviation emr, excess mixing ratio. The percent column for each compound compares the compounds excess mixing ratio to that of CO as a percentage.

[b]Meters above ground level; to convert to meters above sea level, add ~ 70 m.

[c]Time is local Alaskan time.

[d]The uncertainty in smoke age is in parentheses.

[e]The initial emission ratio to CO (as a percentage) for comparison to the downwind percentages.

Table 7. Emission Ratios, Emission Factors, and Total Emissions Estimates for Fires in the Alaskan and Global Boreal Forest[a]

		Emission Ratios As Percent of CO_2			Emission Ratios As Percent of CO									
					Hydrocarbons						Acids			
	MCE	CO_2	CO	NO	CH_4	C_2H_6	C_2H_4	C_2H_2	C_3H_6	HCHO	Formic	Acetic	CH_3OH	NH_3
Alaskan fires														
Wildfire B280	0.916		9.17	...	6.01	...	2.49	0.27	...	2.07	0.58	1.65	1.32	2.57
Wildfire B349	0.929		7.6	0.14	4.89	...	1.39	0.28	...	1.72	0.52	0.87	1.33	1.22
Wildfire B309	0.917		9.1	0.13	5.45	...	1.88	0.25	...	1.78	0.77	1.15	1.4	1.22
Nance et al. [1993]	0.928		7.81	...	5.7	0.73	...	0.35	0.41	...	...	...	...	1.3
Average MCE	0.923		...	...	...	...	...	...	...	...	...	...	...	...
Average emission ratio			8.42	0.14	5.51	0.73	1.92	0.29	0.41	1.86	0.62	1.22	1.35	1.58
Emission factors, g kg^{-1}[b]		1660	88.8	1.54	2.79	0.66	1.80	0.24	0.51	1.85	0.99	2.42	1.41	0.86
Emission factors, g kg^{-1}[c]		...	...	...	...	...	...	...	...	2.29	...	3.61	1.66	...
Estimates of Total Alaskan Fire Emissions of Each Compound in Teragrams														
Estimate type														
Annual average (1988-1997)		26.1	1.40	0.024	0.044	0.010	0.028	0.004	0.008	0.029	0.016	0.038	0.022	0.013
1997		45.9	2.46	0.043	0.077	0.018	0.050	0.007	0.014	0.051	0.027	0.067	0.039	0.024
Other Measurements of Fire-Average Emission Factors in the Global Boreal Forest														
Study														
Hegg et al. [1990] (Hardiman Fire)		1664	82	3.3[d]	1.9	0.45	...	0.31	0.58	...	...	...	...	0.1
Hegg et al. [1990] (Battersby Fire)		1508	175	1.05[d]	5.6	0.57	...	0.33	0.9	...	...	...	...	...
Radke et al. [1991] (Hill Fire, airborne study)		1646	90	...	4.2	0.48	...	0.25	0.65	...	...	...	...	...
Susott et al. [1991] (Hill Fire, tower-based study)		1648	99.6	...	...	...	...	...	...	...	...	...	...	...
Cofer et al. [1996] (Bor Island Crown Fire)		1475	180	...	4.2	...	...	...	...	...	...	...	...	...
Yokelson et al. [1997][e]		1142	153	...	5.3	0.9	1.1	0.1	2.1	1.8	1.4	7.7	2.5	4.5
Estimates of Total Boreal Forest Fire Emissions of Each Compound in Teragrams														
Estimate type														
Annual average		536	28.7	0.50	0.90	0.21	0.58	0.08	0.16	0.60	0.32	0.78	0.46	0.28
Upper limit[f]		1992	213.1	3.7	6.7	1.6	4.3	0.6	1.2	4.4	2.4	5.8	3.4	2.1

[a]See discussion insection 3.5.

[b]The arithmetic average of the emission factors from Tables 2-4 (this work) and *Nance et al.* [1993] (Table 2). The average standard deviation in the average emission ratios is 15%.

[c]Calculated from the average MCE and the plots in Figure 3a-3c.

[d]These entries are measurements of NO_x ($NO + NO_2$).

[e]From laboratory measurements of smoldering organic soils (average MCE = 0.83); the emission factor is based on the carbon percentage of the bulk material including inorganic matter.

[f]Assuming 20 million ha burned, fuel consumption = 60 t ha^{-1}, and doubling the non-CO_2, average, Alaskan emission factors.

factors are larger than those calculated from the in situ data since the Alaska data lie just below the linear fit shown in the plots in Figure 3. In this type of situation, the locally measured emission factors are preferred to the model predictions, which are more appropriate when specific, regional emission factors were not measured reliably.

The emission factors in Table 7 can be coupled with estimates of area burned and fuel consumption to estimate total fire emissions at various geographic or temporal scales. For the state of Alaska, we use area-burned estimates based on aerial surveys conducted by the Alaska Fire Service (AFS) [*Alaska Fire Service*, 1997]. The average, annual burned area (1988-1997), based on AFS data, is 429,000 ± 435,000 ha (1σ). (The large standard deviation is due to the large range (~2 orders of magnitude) in annual area burned.) The AFS estimate for area-burned during 1997 (the year this study was conducted) is 753,563 ha, which is the third largest total during the 1988-1997 time period. Several estimates of fuel consumption in Alaska are available. *French et al.* [1996] made detailed measurements of carbon release by a boreal forest fire in Alaska and developed a model that predicts a carbon release between 8 and 40 t C ha^{-1} depending on the time of year and vegetation type. *Kasischke et al.* [1995] derived estimates of annual average carbon release for Alaskan fires of 25.4 t C ha^{-1} (1990) and 30.0 t C ha^{-1} (1991). In recent studies, Kasischke and coworkers measured fuel-type-specific carbon stocks on paired burned and unburned sites near Tok, Alaska. They addressed burn variability with vegetation and remote sensing information and estimated the fire-average carbon release for two fires: 21.4 t C ha^{-1} [*Kasischke et al.*, 2000a] and 30.0 t C ha^{-1} [*Kasischke et al.*, 2000b]. Finally, prefire and postfire biomass loading was measured for a representative section of wildfire B309 that burned on June 28, 1997 (1 day after our airborne sampling). The total biomass consumption was 36.7 ± 7 (2σ) t ha^{-1} (S. Drury, manuscript in preparation, 2000). Based on these biomass consumption measurements, we make a conservative estimate of total emissions by assuming that 36 ±7 t ha^{-1} is the fuel consumption for Alaskan fires. Multiplying this fuel consumption value by the AFS area-burned estimates and our Alaskan, boreal forest emission factors yields the conservative annual average and 1997 total-Alaskan emissions estimates shown in Table 7. The estimated 46 ± 11 (1σ) Tg of CO_2 emitted by the 1997 Alaska fires is comparable to the 36 Tg of CO_2 released by the entire country of Norway (annual average 1989-1995) as estimated by the Norwegian Ministry of the Environment per International Panel on Climate Change guidelines (http://odin.dep.no/md/publ/climate/3.html). This illustrates that fires are a relatively important source of trace gases compared to other sources located at latitudes > ~60°N.

Scaling emissions estimates to the global boreal forest entails using less certain area-burned estimates, and it is not clear how well the emission factors and the fuel consumption value we assumed for Alaska represent forest fires in the whole, circumpolar boreal region. Recent estimates of the annual average burned area in the global boreal forest include 8.8 million ha [*Kasischke et al.*, 1999] and 14.6 million ha [*Conard and Ivanova*, 1997]. Fuel consumption measurements outside Alaska include 38 t ha^{-1} due to a prescribed crown fire at Bor Forest Island in Siberia [*FIRESCAN Science Team*, 1996] and 42.7 t ha^{-1} for a prescribed crown fire in the Northwest Territories, Canada [*Cofer et al.*, 1998]. According to *Kasischke et al.* [1999], fuel consumption for boreal forest fires is normally 10-20 t ha^{-1} but can be as large as 50-60 t ha^{-1} in drought years when substantial amounts of organic soils and canopy fuels burn. Both *Stocks* [1991] and *Cahoon et al.* [1994, 1996] assumed an average fuel consumption of 25 t ha^{-1} for the global boreal forest.

A few measurements of fire-average emission factors have been made in Canadian and Russian boreal forests. *Hegg et al.* [1990] and *Radke et al.* [1991] made airborne measurements of the fire-average emission factors on three fires in Ontario for NO_x, NH_3, and a variety of gases sampled in stainless steel canisters. For one of these fires, *Susott et al.* [1991] also calculated fire-average emission factors for CO_2 and CO from continuous tower-based measurements of mixing ratios and vertical velocity. *Cofer et al.* [1989, 1998] reported "spot," airborne measurements of emission factors obtained during different combustion "phases" of two small, prescribed, "crown" fires and some larger "slash" fires. However, they reported fire-average emission factors only for the Bor Island Crown Fire [*Cofer et al.*, 1996]. The fire-average emission factors from the above studies are shown in Table 7 for the compounds that we also measured. In Table 7 we note that the CO emission factors for the Battersby Fire (which was very intense) and the Bor Island Crown Fire are nearly identical and about twice as large as the CO emission factors for the Hill Fire (which was extremely intense), the Hardiman Fire, and our Alaskan fires. There is considerable controversy in the literature on the relative area burned by crown and surface fires, and it is also not clear if the emissions from these two types of fires are different. The emission factors measured by *Yokelson et al.* [1997] for "smoldering compounds" released from smoldering, Alaskan organic soils are also larger than our average, Alaskan, boreal forest fire emission factors (Table 7). In summary, under extreme drought conditions, fires probably consume more canopy fuels and more organic soils. Thus, especially in severe fire years, the real global, boreal forest, average emission factor for CO and some other gases might be higher than what we (and *Nance et al.* [1993]) measured in Alaska.

We now incorporate the above observations into conservative and upper-limit estimates of the trace gas emissions from the global boreal forest. To calculate a conservative estimate for average annual emissions, we assume that 8.8 million ha of boreal forest are burned with an average biomass consumption of 36.7 t ha^{-1}, and we use our Alaskan, boreal forest emission factors to obtain the annual average, total emissions shown in Table 7. We then calculate an upper-limit estimate by assuming 20 million ha burned, fuel consumption of 60 t ha^{-1} [*Kasischke* et al., 1999], and doubling the emission factors for compounds other than CO_2. The annual CO emissions in the hypothetical, upper-limit estimate (bottom row, Table 7) are ~7.5 times larger than in the conservative estimate and approach 25% of the total, annual CO emissions from all global biomass burning [*Crutzen and Andreae*, 1990]. Of course, what are currently projected peak emissions could become average emissions in the future if this region has the sensitivity to global warming discussed earlier. In any event, these emissions are released within 4-5 months in areas with relatively small anthropogenic sources and many are reactive trace gases. Therefore they are likely to have significant regional effects.

4. Conclusions

Airborne FTIR measurements of the trace gas emissions from four Alaskan, boreal zone wildfires yielded excess mixing ratios for many of the major smoke constituents: water, ozone, carbon dioxide, nitric oxide, carbon monoxide, methane, formaldehyde, acetic acid, formic acid, methanol, ethylene, acetylene, ammonia, and hydrogen cyanide. The emission ratios to carbon monoxide for the oxygenated organic compounds formaldehyde, acetic acid, formic acid, and methanol were each ~1-2% and in good agreement with our North Carolina airborne study and our extensive results from laboratory fires in hardwood, softwood, grass, and organic soil fuels. Taken together, these results suggest that fires are a major global source of oxygenated compounds. For methanol, acetic acid, and formaldehyde, a plot of the fire emission factors versus MCE for all our FTIR-based measurements in the laboratory and in the field, in diverse aboveground fuels, can be fit with a highly correlated regression line specific to each compound. The linear regression fit to our data can be used for estimating emissions of these difficult to measure compounds from fires where no reliable, regional measurements have been made. Our Alaska data also fit a linear equation for predicting the NH_3/NO_x molar emission ratio as a function of fire MCE. This equation fits results from a range of global fires and investigators and can be used to estimate the major reactive nitrogen emissions. Downwind smoke samples that had aged in the upper part of the plume for 2.2 ± 1 hours had $\Delta O_3/\Delta CO$ ratios of 7.9 ± 2.4% resulting from O_3 formation rates of ~50 ppbv h^{-1}. Downwind samples obtained well inside another plume, and of similar age, did not have detectable O_3, but did have $\Delta NH_3/\Delta CO$ ratios about 1/3 of the initial value. $\Delta HCOOH/\Delta CO$ and $\Delta CH_3COOH/\Delta CO$ usually increased about a factor of 2 over the same timescale in samples from both plumes. Observations such as these could be useful in developing photochemical plume models and linking source strength measurements with haze layer measurements. The emission factors we measured in Alaska were combined with those from another Alaskan fire study to derive a substantial set of average, Alaskan, boreal forest fire emission factors. Using these emission factors we confirm that emissions from wildfires are one of the main sources of trace gases located at high latitudes. Boreal fire emissions are normally only a few percent of global fire emissions. However, boreal forest fire CO emissions might account for as much as 25% of the global CO emissions from all fires during an extremely severe, boreal zone fire year.

Acknowledgments. This research was supported by funds provided by the U.S. Department of the Interior Bureau of Land Management under grant BLM (95-IA-139), the National Science Foundation under grants ATM-9631219 and ATM-9900494, and by funds provided by the Rocky Mountain Research Station, Forest Service, U.S. Department of Agriculture (INT-96079-RJVA and INT-97082-RJVA). The authors thank the Alaska Fire Service, Fairbanks for hosting and supporting our air operations in Alaska; our pilots Lamont Humber, Edward Kral, and Clarence Shockly; the staff of the Forest Service Aviation and Fire Management office in Missoula for arranging our use of the Forest Service King Air; John Palmer of the Alaska BLM for providing the remote automated weather station data; and Larry Oolman of the University of Wyoming for providing the upper air sonde and surface weather data for Alaska. Tim Hammond from the Alaska BLM provided vegetation maps, fire history data, and invaluable GIS assistance.

References

Alaska Fire Service, Draft Fire History, Bureau of Land Management, Ft. Wainwright, Alaska, 1997.

Andreae, M. O., et al., Biomass-burning emissions and associated haze layers over Amazonia, *J. Geophys. Res.*, *93*, 1509-1527, 1988.

Andreae, M. O., B. E. Anderson, D. R. Blake, J. D. Bradshaw, J. E. Collins, G. L. Gregory, G. W. Sachse, and M. C. Shipham, Influence of plumes from biomass burning on atmospheric chemistry over the equatorial and tropical South Atlantic during CITE 3, *J. Geophys. Res.*, *99*, 12,793-12,808, 1994.

Apps, M. J., W. A. Kurz, R. L. Luxmoore, L. O. Nilsson, R. A. Sedjo, R. Schmidt, L. G. Simpson, and T. S. Vinson, Boreal forests and tundra, *Water Air Soil Pollut.*, *70*, 39-53, 1993.

Birdsey, R. A., Carbon storage and accumulation in US forest ecosystems, *Gen. Tech. Rep. WO-59*, 51 pp., U. S. Dep. of Agric. For. Serv., Washington, D. C., 1992.

Bradshaw, J. D., R. W. Talbot, H. B. Singh, D. R. Blake, G. W. Sachse, and A. Bachmeier, Summertime tropospheric distribution of reactive odd-nitrogen compounds over Canada (abstract), *Eos Trans. AGU*, *72* (17), Spring Meet. Suppl., 74, 1991.

Brocard, D., C. Lacaux, J.-P. Lacaux, G. Kouadio, and V. Yoboué, Emissions from the combustion of biofuels in western Africa, in *Biomass Burning and Global Change*, edited by J. S. Levine, pp. 350-360, MIT Press, Cambridge, Mass., 1996.

Cahoon, D. R., Jr., B. J. Stocks, J. S. Levine, W. R. Cofer III, and J. M. Pierson, Satellite analysis of the severe 1987 forest fires in northern China and southeastern Siberia, *J. Geophys. Res.*, *99*, 18,627-18,638, 1994.

Cahoon, D. R., Jr., B. J. Stocks, J. S. Levine, W. R. Cofer III, and J. A. Barber, Monitoring the 1992 forest fires in the boreal ecosystem using NOAA AVHRR satellite imagery, in *Biomass Burning and Global Change*, edited by J. S. Levine, pp. 795-801, MIT Press, Cambridge, Mass., 1996.

Chapin, F. S., III, and G. R. Shaver, Arctic, in *Physiological Ecology of North American Plant Communities*, edited by B. F. Chabot and H. A. Mooney, pp. 16-40, Chapman and Hall, New York, 1985.

Chatfield, R. B., and A. C. Delaney, Convection links biomass burning to increased tropical ozone: However, models will tend to overpredict O_3, *J. Geophys. Res.*, *95*, 18,473-18,488, 1990.

Chatfield, R. B., J. A. Vastano, H. B. Singh, and G. W. Sachse, A general model of how fire emissions and chemistry produce African/oceanic plumes (O_3, CO, PAN, smoke) in TRACE A, *J. Geophys. Res.*, *101*, 24, 279-24,306, 1996.

Cofer, W. R., III, J. S. Levine, D. I. Sebacher, E. L. Winstead, P. J. Riggan, B. J. Stocks, J. A. Brass, V. G. Ambrosia, and P. J. Boston, Trace gas emissions from chaparral and boreal forest fires, *J. Geophys. Res.*, *94*, 2255-2259, 1989.

Cofer, W. R., III, E. L. Winstead, B. J. Stocks, L. W. Overbay, J. G. Goldammer, D. R. Cahoon, and J. S. Levine, Emissions from boreal forest fires: Are the atmospheric impacts underestimated?, in *Biomass Burning and Global Change*, edited by J. S. Levine, pp. 834-839, MIT Press, Cambridge, Mass., 1996.

Cofer, W. R., III, E. L. Winstead, B. J. Stocks, J. G. Goldammer, and D. R. Cahoon, Crown fire emissions of CO_2, CO, H_2, CH_4, and TNMHC from a dense jack pine boreal forest fire, *Geophys. Res. Lett.*, *25*, 3919-3922, 1998.

Conard, S. G., and G. A. Ivanova, Wildfire in Russian boreal forests: Potential impacts of fire regime characteristics on emissions and global carbon balance estimates, *Environ. Pollut.*, *98*, 305-313, 1997.

Crutzen, P. J., and M. O. Andreae, Biomass burning in the tropics: Impact on atmospheric chemistry and biogeochemical cycles, *Science*, *250*, 1669-1678, 1990.

Fan, S.-M., D. J. Jacob, D. L. Mauzerall, J. D. Bradshaw, S. T. Sandholm, D. R. Blake, H. B. Singh, R. W. Talbot, G. L. Gregory, and G. W. Sachse, Photochemistry of reactive nitrogen in the subarctic troposphere in summer 1990: Observations and modeling, *J. Geophys. Res.*, *99*, 16,867-16,878, 1994.

Finlayson-Pitts, B. J., and J. N. Pitts Jr., *Atmospheric Chemistry: Fundamentals and Experimental Techniques*, John Wiley, New York, 1986.

FIRESCAN Science Team, Fire in ecosystems of boreal Eurasia: The

Bor forest island fire experiment fire research campaign Asia-North (FIRESCAN), in *Biomass Burning and Global Change*, edited by J. S. Levine, pp. 848-873, MIT Press, Cambridge, Mass., 1996.

Fishman, J., K. Fakhruzzaman, B. Cros, and D. Nganga, Identification of widespread pollution in the Southern Hemisphere deduced from satellite analyses, *Science*, *252*, 1693-1696, 1991.

Flannigan, M. D., and C. E. Van Wagner, Climate change and wildfire in Canada, *Can. J. For. Res.*, *21*, 66-72, 1991.

French, N. H. F., E. S. Kasischke, R. D. Johnson, L. L. Bourgeau-Chavez, A. L. Frick, and S. Ustin, Estimating fire-related carbon flux in Alaskan boreal forests using multisensor remote-sensing data, in *Biomass Burning and Global Change*, edited by J. S. Levine, pp. 808-826, MIT Press, Cambridge, Mass., 1996.

Goode, J. G., R. J. Yokelson, R. A. Susott, and D. E. Ward, Trace gas emissions from laboratory biomass fires measured by open-path Fourier transform infrared spectroscopy: Fires in grass and surface fuels, *J. Geophys. Res.*, *104*, 21,237-21,245, 1999.

Griffith, D. W. T., Synthetic calibration and quantitative analysis of gas-phase FTIR spectra, *Appl. Spectrosc.*, *50*, 59-70, 1996.

Griffith, D. W. T., W. G. Mankin, M. T. Coffey, D. E. Ward, and A. Riebau, FTIR remote sensing of biomass burning emissions of CO_2, CO, CH_4, CH_2O, NO, NO_2, NH_3 and N_2O, in *Global Biomass Burning: Atmospheric, Climatic, and Biospheric Implications*, edited by J. S. Levine, pp. 230-239, MIT Press, Cambridge, Mass., 1991.

Hao, W. M., and M.-H. Liu, Spatial and temporal distribution of tropical biomass burning, *Global Biogeochem. Cycles*, *8*, 495-503, 1994.

Hegg, D. A., L. F. Radke, P. V. Hobbs, R. A. Rasmussen, and P. J. Riggan, Emissions of some trace gases from some biomass fires, *J. Geophys. Res.*, *95*, 5669-5675, 1990.

Holzinger, R., C. Warneke, A. Hansel, A. Jordan, W. Lindinger, D. H. Scharffe, G. Schade, and P. J. Crutzen, Biomass burning as a source of formaldehyde, acetaldehyde, methanol, acetone, acetonitrile, and hydrogen cyanide, *Geophys. Res. Lett.*, *26*, 1161-1164, 1999.

Hurst, D. F., D. W. T. Griffith, and G. D. Cook, Trace gas emissions from biomass burning in tropical Australian savannas, *J. Geophys. Res.*, *99*, 16,441-16,456, 1994.

Jacob, D. J., et al., Summertime photochemistry of the troposphere at high northern latitudes, *J. Geophys. Res.*, *97*, 16,421-16,431, 1992.

Jacob, D. J., et al., Origin of ozone and NO_x in the tropical troposphere: A photochemical analysis of aircraft observations over the South Atlantic basin, *J. Geophys. Res.*, *101*, 24,235-24,250, 1996.

Kasischke, E. S., N. H. F. French, L. L. Bourgeau-Chavez, and N. L. Christensen Jr., Estimating release of carbon from 1990 and 1991 forest fires in Alaska, *J. Geophys. Res.*, *100*, 2941-2951, 1995.

Kasischke, E. S., K. Bergen, R. Fennimore, F. Sotelo, G. Stephens, A. Janetos, and H. H. Shugart, Satellite imagery gives clear picture of Russia's boreal forest fires, *Eos Trans. AGU*, *80*, 141, 147, 1999.

Kasischke, E. S., K. P. O'Neill, N. H. F. French, and L. L. Bourgeau-Chavez, Controls on patterns of biomass burning in Alaskan boreal forests, in *Fire, Climate Change and Carbon Cycling in the Boreal Forest, Ecol. Stud. Ser.*, edited by E. S. Kasischke and B. J. Stocks, pp. 173-196, Springer-Verlag, New York, 2000a.

Kasischke, E. S., N. H. F. French, and L. L. Bourgeau-Chavez, Using satellite data to monitor fire-related processes in boreal forests, in *Fire, Climate Change and Carbon Cycling in the Boreal Forest, Ecol. Stud. Ser.*, edited by E. S. Kasischke and B. J. Stocks, pp. 406-422, Springer-Verlag, New York, 2000b.

Lacaux, J. P., D. Brocard, C. Lacaux, R. Delmas, A. Brou, V. Yoboué, and M. Koffi, Traditional charcoal making: An important source of atmospheric pollution in the African tropics, *Atmos. Res.*, *35*, 71-76, 1994.

Lelieveld, J., P. J. Crutzen, D. J. Jacob, and A. M. Thompson, Modeling of biomass burning influences on tropospheric ozone, in *Fire in Southern African Savannas: Ecological and Atmospheric Perspectives*, edited by B. W. van Wilgen et al., pp. 217-238, Witwatersrand Univ. Press, Johannesburg, South Africa, 1997.

Lindesay, J. A., M. O. Andreae, J. G. Goldammer, G. Harris, H. J. Annegarn, M. Garstang, R. J. Scholes, and B. W. van Wilgen, International Geosphere-Biosphere Programme/International Global Atmospheric Chemistry SAFARI-92 field experiment: Background and overview, *J. Geophys. Res.*, *101*, 23,521-23,530, 1996.

Little, R. J. A., and D. B. Rubin, *Statistical Analysis With Missing Data*, 152 pp., John Wiley, New York, 1987.

Lobert, J. M., D. H. Scharffe, W. M. Hao, T. A. Kuhlbusch, R. Seuwen, P. Warneck, and P. J. Crutzen, Experimental evaluation of biomass burning emissions: Nitrogen and carbon containing compounds, in *Global Biomass Burning: Atmospheric, Climatic, and Biospheric Implications*, edited by J. S. Levine, pp. 289-304, MIT Press, Cambridge, Mass., 1991.

Mauzerall, D. L., D. J. Jacob, S.-M. Fan, J. D. Bradshaw, G. L. Gregory, G. W. Sachse, and D. R. Blake, Origin of tropospheric ozone at remote high northern latitudes in summer, *J. Geophys. Res.*, *101*, 4175-4188, 1996.

Mauzerall, D. L., J. A. Logan, D. J. Jacob, B. E. Anderson, D. R. Blake, J. D. Bradshaw, B. Heikes, G. W. Sachse, H. Singh, and R. Talbot, Photochemistry in biomass burning plumes and implications for tropospheric ozone over the tropical South Atlantic, *J. Geophys. Res.*, *103*, 8401-8423, 1998.

McKenzie, L. M., W. M. Hao, G. N. Richards, and D. E. Ward, Measurement and modeling of air toxins from smoldering combustion of biomass, *Environ. Sci. Technol.*, *29*, 2047-2054, 1995.

Nance, J. D., P. V. Hobbs, L. F. Radke, and D. E. Ward, Airborne measurements of gases and particles from an Alaskan wildfire, *J. Geophys. Res.*, *98*, 14,873-14,882, 1993.

Office of Fire and Aviation Management, Wildfire statistics, 1997, Bur. of Land Manage., Boise, Idaho, April 1998.

Perrin, A., C. P. Rinsland, and A. Goldman, Spectral parameters for the ν_6 region of HCOOH and its measurement in the infrared tropospheric spectrum, *J. Geophys. Res.*, *104*, 18,661-18,666, 1999.

Radke, L. F., D. A. Hegg, P. V. Hobbs, J. D. Nance, J. H. Lyons, K. K. Laursen, R. E. Weiss, P. J. Riggan, and D. E. Ward, Particulate and trace gas emissions from large biomass fires in North America, in *Global Biomass Burning: Atmospheric, Climatic, and Biospheric Implications*, edited by J. S. Levine, pp. 209-224, MIT Press, Cambridge, Mass., 1991.

Senff, C. J., R. M. Hardesty, R. J. Alvarez II, and S. D. Mayor, Airborne LIDAR characterization of power plant plumes during the 1995 Southern Oxidants Study, *J. Geophys. Res.*, *103*, 31,173-31,189, 1998.

Singh, H. B., Reactive nitrogen distribution and photochemistry during ABLE 3B (abstract), *Eos Trans. AGU*, *72* (17), Spring Meet Suppl., 74, 1991.

Singh, H. B., et al., Summertime distribution of PAN and other reactive nitrogen species in the northern high-latitude atmosphere of eastern Canada, *J. Geophys. Res.*, *99*, 1821-1836, 1994.

Singh, H. B., M. Kanakidou, P. J. Crutzen, and D. J. Jacob, High concentrations and photochemical fate of oxygenated hydrocarbons in the global troposphere, *Nature*, *378*, 50-54, 1995.

Smith, T. M., W. P. Cramer, R. K. Dixon, R. Leemans, R. P. Neilson, and A. M. Solomon, The global terrestrial carbon cycle, *Water Air Soil Pollut.*, *70*, 19-37, 1993.

Stith, J. L., L. F. Radke, and P. V. Hobbs, Particle emissions and the production of ozone and nitrogen oxides from the burning of forest slash, *Atmos. Environ.*, *15*, 73-82, 1981.

Stocks, B. J., The extent and impact of forest fires in northern circumpolar countries, in *Global Biomass Burning: Atmospheric, Climatic, and Biospheric Implications*, edited by J. S. Levine, pp. 197-202, MIT Press, Cambridge, Mass., 1991.

Stocks, B. J., et al., Climate change and forest fire potential in Russian and Canadian boreal forests, *Clim. Change*, *38*, 1-13, 1998.

Susott, R. A., D. E. Ward, R. E. Babbitt, and D. J. Latham, Measurement of trace gas emissions and combustion characteristics for a mass fire, in *Global Biomass Burning: Atmospheric, Climatic, and Biospheric Implications*, edited by J. S. Levine, pp. 245-257, MIT Press, Cambridge, Mass., 1991.

Susott, R. A., G. J. Olbu, S. P. Baker, D. E. Ward, J. B. Kauffman, and R. Shea, Carbon, hydrogen, nitrogen, and thermogravimetric

analysis of tropical ecosystem biomass, in *Biomass Burning and Global Change*, edited by J. S. Levine, pp. 350-360, MIT Press, Cambridge, Mass, 1996.

Talbot, R. W., K. M. Beecher, R. C. Harriss, and W. R. Cofer III, Atmospheric geochemistry of formic and acetic acids at a midlatitude temperate site, *J. Geophys. Res.*, *93*, 1638-1652, 1988.

Ward, D. E., and L. F. Radke, Emissions measurements from vegetation fires: A comparative evaluation of methods and results, in *Fire in the Environment: The Ecological, Atmospheric and Climatic Importance of Vegetation Fires*, edited by P. J. Crutzen and J. G. Goldammer, pp. 53-76, John Wiley, New York, 1993.

Ward, D. E., R. A. Susott, A. P. Waggoner, P. V. Hobbs, and J. D. Nance, Emission factor measurements for two fires in British Columbia compared with results for Oregon and Washington, paper presented at Pacific Northwest International Section of the Air and Waste Management Association Meeting, Air and Waste Manage. Assoc.,Bellevue, Wash., Nov., 11-13, 1992.

Webster, C. R., R. D. May, C. A. Trimble, R. G. Chave, and J. Kendall, Aircraft (ER-2) laser infrared absorption spectrometer (ALIAS) for in situ stratospheric measurements of HCl, N_2O, CH_4, NO_2, and HNO_3, *Appl. Opt.*, *33*, 454-472, 1994.

Wennberg, P. O., et al., Hydrogen radicals, nitrogen radicals, and the production of O_3 in the upper troposphere, *Science*, *279*, 49-53, 1998.

Wofsy, S. C., et al., Atmospheric chemistry in the arctic and subarctic: Influence of natural fires, industrial emissions, and stratospheric inputs, *J. Geophys. Res.*, *97*, 16,731-16,746, 1992.

Worden, H., R. Beer, and C. P. Rinsland, Airborne infrared spectroscopy of 1994 western wildfires, *J. Geophys. Res.*, *102*, 1287-1299, 1997.

Wotton, B. M., and M. D. Flannigan, Length of fire season in a changing climate, *For. Chron.*, *69*, 187-192, 1993.

Yokelson, R. J., D. W. T. Griffith, J. B. Burkholder, and D. E. Ward, Accuracy and advantages of synthetic calibration of smoke spectra, in *Optical Remote Sensing for Environmental and Process Monitoring*, pp. 365-376, Air and Waste Manage. Assoc., Pittsburgh, Pa., 1996a.

Yokelson, R. J., D. W. T. Griffith, and D. E. Ward, Open-path Fourier transform infrared studies of large-scale laboratory biomass fires, *J. Geophys. Res.*, *101*, 21,067-21,080, 1996b.

Yokelson, R. J., D. E. Ward, R. A. Susott, J. Reardon, and D. W. T. Griffith, Emissions from smoldering combustion of biomass measured by open-path Fourier transform infrared spectroscopy, *J. Geophys. Res.*, *102*, 18,865-18,877, 1997.

Yokelson, R. J., D. W. T. Griffith, R. A. Susott, and D. E. Ward, Spectroscopic studies of biomass fire emissions, in *Proceedings of the 13th Conference on Fire and Forest Meteorology*, vol. 1, pp. 183-196, Int. Assoc. of Wildland Fire, Fairfield, Wash., 1998.

Yokelson , R. J., J. G. Goode, I. Bertschi, R. A. Susott, R. E. Babbitt, D. E. Ward, W. M. Hao, D. D. Wade, and D. W. T. Griffith, Emissions of formaldehyde, acetic acid, methanol, and other trace gases from biomass fires in North Carolina measured by airborne Fourier transform infrared spectroscopy (AFTIR), *J. Geophys. Res.*, *104*, 30,109-30,125, 1999.

R. E. Babbitt, M. A. Davies, W. M. Hao, R. A. Susott, and D. E. Ward, USDA Forest Service, Rocky Mountain Research Station Fire Sciences Laboratory, Missoula, MT 59807.

J. G. Goode, Bruker Optics, Inc., 19 Fortune Drive, Manning Park, Billerica, MA 01821.

R. J. Yokelson (corresponding author), Department of Chemistry, University of Montana, Missoula, MT 59812. (byok@selway.umt.edu)

(Received January 21, 2000; revised April 19, 2000; accepted May 8, 2000.)